$SMART_{LD}$ (SMALL AIRCRAFT RISK TECHNOLOGY –LINEAR DAMAGE) TECHNOLOGY AND CASE STUDIES APPLICATIONS

J.D. OCAMPO, H.R. MILLWATER

University of Texas at San Antonio, San Antonio, TX, 78249

ABSTRACT

This research describes the probabilistic methodology utilized for a computer software program that performs risk assessment of small airplanes. A risk assessment evaluation of the continued operational safety of the general aviation (GA) fleet can provide important insight to the criticality/severity of a potentially serious structural issue. The main objective was to develop a comprehensive probabilistic methodology such that Federal Aviation Administration (FAA) engineers can use to conduct a risk assessment of GA structural issues in support of policy decisions. The methodology and computer software encompass the required elements for a structural integrity evaluation and consider real-world airplane-to-airplane and flight-to-flight variations to make a realistic risk assessment of an aircraft structural detail.

This work includes the development of probability distributions of relevant inputs (PSN Curves, Miner's Damage Coefficients, Flight lengths, Aircraft Speeds, Stresses, etc.) to obtain a realistic risk assessment. Failure is determined using Miner's damage index with the index calibrated from simulations of variable amplitude tests. Monte Carlo sampling is used to determine the structural probability-of-failure, or the mean and standard deviation of the flights- and hours-to-failure, the hazard function and conduct a sensitivity analysis

Two FAA case studies are presented to demonstrate the methodology. The studies include a high performance single-engine airplane with 4,000 pounds of maximum take off weight considered in single usage (Single Engine Unpressurized Executive Usage) and a twin engine airplane with 36,000 pounds of maximum take off weight considered in mix usage (Twin Engine General Usage and Twin Engine Instructional Usage). The results are post-processed to

predict the risk of failure and the associated sensitivities. The sensitivities indicate the relative importance of the inputs on the life estimation.

NOMENCLATURE

A, B, C, D	Constants for polynomial P-S-N curve
a_n	Incremental normal acceleration (in delta g)
a_{nLLF}	Load limit factor
d	Diameter
e	Residuals
F_{ν_1,ν_2}	F-distribution with ν_1 and ν_2 degrees of freedom
g	Load factor
k	Test data points
K_{tb}	Bearing stress concentration factor
K_{tg}	Stress concentration factor based on gross stress
LT	Load transfer
N	Fatigue life
$P, \Delta P$	Force
S	Cyclic stress
S_m	Mean stress
S_a	Alternating stress
t	Thickness
w	Width
X	$Log(S)$
Y	$Log(N)$
Z	Random realization
α, β, θ	Empirical factors
ρ	Pearson correlation
$\hat{\sigma}^2$	Variance
σ	Standard deviation

ASTM	American Society for Testing and Materials
CDF	Cumulative Distribution Function
COV	Coefficient of Variation
D	Damage Index
FAA	Federal Aviation Administration
NASA	National Aeronautics and Space Administration
PDF	Probability Density Function
POF	probability-of-failure
P-S-N	Probabilistic Stress-Life
S-N	Stress-Life
SSF	Stress Severity Factor
V-G/VGH	Velocity-G's/Velocity-Gs-Altitude

INTRODUCTION

In 1991, Congress mandated that the Federal Aviation Administration (FAA) establish an Aging Aircraft Program. The focus of this program was age-related structural problems with airplanes used in public transportation. At the time, Congress excluded the general aviation (GA) fleet from the mandate. However, the FAA determined that as the GA fleet continues to age, there is a concern about ensuring the continued airworthiness of the diverse GA fleet. To guide future efforts in addressing the effects of aging on GA airplanes, the Small Airplane Directorate developed an FAA Aging GA Roadmap that serves as a guide to proactively manage the overall airworthiness of aging GA airplanes. One of the four major focus areas of the Roadmap is data-driven risk assessment and risk management. As a result, a research and development program was undertaken to develop the required methodology, computer software, and supporting data to conduct structural risk assessments.

The US military has developed a probabilistic methodology to augment the traditional damage tolerance analysis where appropriate, particularly for aging aircraft. The PROF software was developed with a capability to consider variability in the initial crack size, fracture toughness, maximum load, probability-of-detection curves and inspection schedules to compute the probability-of-failure per flight [1]. The probabilistic methodology can be used to assess the effects of inspections on reducing the probability-of-failure and for setting inspection schedules

[2]. The aircraft gas turbine engine community has developed a risk assessment methodology for Metallurgical defects due to inclusions [3].

A risk assessment evaluation of the continued operational safety of the GA fleet can provide important insight to the criticality/severity of a potentially serious structural issue. As such, the methodology and a computer code, "SMART|LD" were developed to address risk assessment and risk management of GA structural issues. This information can be used to formulate a proactive approach to enable a nonbiased review of data to assure airworthiness.

The methodology requires probabilistic information on loading and material behavior. Therefore, the random variable distributions for loading (gust and maneuver loads, sink rate, flight velocity-duration, and flight weight-duration), and material behavior (probabilistic stress-life (P-S-N) curves from constant amplitude tests) were developed. The stress severity factor concept was used to account for localized stress concentrations and structural geometry.

Failure is computed based on Miner's linear damage rule. Although there are advantages of nonlinear damage rules, they require calibration of constants for different materials. Due to the large variety in material pedigree for general aviation aircraft, it was determined that Miner's rule is the most generally applicable and should be used. However, it is known that failure under variable amplitude loading may occur for damage values significantly different than one; therefore, a provision was made such that a probabilistic user-defined damage index can be used. In addition, the methodology can be used to calibrate a distribution for minors damage index based on variable aptitude tests.

A Monte Carlo simulation is used to calculate the mean and standard deviation of the hours/flight-to-failure, the probability-of-failure, and also conduct sensitivity analysis. Useful outputs include histogram plots, the hazard function, and scatter plots for random variables. Correlation coefficients are computed to indicate the relative importance of the random variables.

The objective of this paper is to describe the methodology in detail, the development of the requisite probability distributions, and the application to two different GA case studies.

METHODOLOGY OVERVIEW

The methodology in this work encompasses the required elements necessary to conduct a structural integrity evaluation and considers real-world airplane-to-airplane and flight-to-flight

variations such that a realistic risk assessment of an aircraft structural detail can be performed. Table 1 shows a summary of the inputs necessary to conduct the risk assessment. A number of the random variables are probabilistic and modeled as random variables.

The One-g stress is the stress measured at the critical location when the airplane is under only the gravitational load. The ground stress is the stress measured at the critical location when the airplane is on the ground.

To perform a risk evaluation, two different methodologies that follow the FAA guidelines used for safe-life evaluation [5] and [8] were incorporated in a computer code. The first methodology called "Damage" calculates the probability distribution and the mean and standard deviation of the flights- and hours-to-failure time. This overall probabilistic methodology is explained step by step as follows:

- Variables such as airplane usage, load limit factors, ground stress, one-g stress, airplane velocity, and flight length are input by the user as shown in Table 1.
- According to the airplane usage specific to general aviation, e.g., single-engine unpressurized instructional usage; the respective data (gust and maneuver exceedance curves, sink rate, and taxi) are loaded from internal libraries.
- Monte Carlo sampling is initiated. For each sample:
    - A realization of the random variables, such as exceedance curves, sink rate velocity, airplane velocity, and flight duration, etc., as shown in Table 1 are generated. A weighted mix of usages is allowed.
    - A characteristic stress spectrum is generated that includes the flight stages: gust, maneuver, taxi, ground-air-ground, and landing and rebound. The methodology process through this point is shown in Figure 1.
    - The local stress severity factor is computed using the loadings, load limit factors, ground stress, one-g stress, and joint geometry.
    - An S-N curve is generated from the probabilistic S-N curve.
    - Based on the stress severity factor and the S-N curve, the damage is calculated for each load pair and accumulated.
    - A realization of Miner's critical damage index is generated.

    - Damage is accumulated for each Monte Carlo sample using Miner's rule until Miner's critical damage index is reached and the flights/hours-to-failure are recorded, as shown in Figure 2.
- When the Monte Carlo sampling is finished, the random variables and flights/hours-to-failure are post-processed to determine the probability distribution of flights/hours-to-failure (probabilities, mean, standard deviation, confidence intervals, hazard function) and to identify the significant random variables using correlation coefficients.

The second methodology, called "Hours" calculates the accumulated damage condition and the probability-of-failure (POF) given a user-defined number of hours flown by the airplane. The methodology is explained step by step as follows:

- Variables such as airplane usage, load limit factors, ground stress, one-g stress, airplane velocity, and flight length are input by the user as shown in Table 1.
- According to the airplane usage specific to general aviation, e.g., single-engine unpressurized instructional usage, the respective data (gust and maneuver exceedance curves, sink rate, and taxi) are loaded from internal libraries.
- Monte Carlo sampling is initiated. For each sample:
    - A realization of the random variables, such as exceedance curves, sink rate velocity, airplane velocity, and flight duration, etc., as shown in Table 1, are generated. A weighted mix of usages is allowed.
    - A characteristic stress spectrum is generated that includes the flight stages: gust, maneuver, taxi, ground-air-ground, and landing and rebound. The methodology process through this point is shown in Figure 1.
    - The local stress severity factor is computed using the loadings, load limit factors, ground stress, one-g stress, and joint geometry.
    - An S-N curve is generated from the probabilistic S-N curve.
    - Based on the stress severity factor and the S-N curve, the damage is calculated for each load pair and accumulated.
    - A realization of Miner's critical damage index is generated.
    - Damage is accumulated for each Monte Carlo sample until the flight hours specified by the user is reached. The accumulated damage is recorded as shown in

Figure 3. If the damage recorded is larger than the random Miner's damage coefficient generated for that sample, a failure is counted.

- When the Monte Carlo sampling is finished, the random variables, the accumulated damage, and the failures are post-processed to obtain the probability-of-failure, percentage damage per flight stage, and the significant random variables.

The load and stress spectrum is a key component of the probabilistic code; a general explanation follows.

Load and Stress Spectrum Generation

During 1962, at the request of the FAA, and upon recommendation of the National Aeronautics and Space Administration (NASA) Committee on Aircraft Operating Problems, the NASA V-G (velocity, normal acceleration)/VGH (velocity, normal acceleration, pressure altitude) General Aviation Program was established [11]. This program recorded gust and maneuver loads, airspeed practices, and other variables for general aviation airplanes to provide a data bank of information for use by airplane designers and evaluators. The program recorded more that 42,155 hours of VGH data of more than 105 airplanes. Tabulated data of the exceedance curves can be found in References [5 and 8]. A probabilistic assessment of exceedance curves can be found Reference [4].

Maneuver and Gust Loads

The data for maneuver and gust loads are presented as the cumulative number of occurrences per nautical mile versus the acceleration fraction (an airplane characteristic defined as the incremental normal acceleration divided by the incremental limit factor). Maneuver and gust use the same methodology to generate load data, so only the gust load methodology is discussed.

The gust spectra in the exceedance curves is expressed in terms of the gust load factor ratio:

$$\frac{a_n}{a_{nLLF}} = \frac{\text{Incremental normal acceleration (in delta g)}}{\text{Load limit factor}} \tag{1}$$

To develop the gust stress spectrum, a sweep through the exceedance curve of acceleration fraction values, see Figure 4, is conducted to account for the possible loads that an airplane faces during a flight. An example is presented for illustration purposes using only four values (0.10, 0.16, 0.22, and 0.28). The values and calculations needed to compute damage due to gust loading are shown in Table 2 with the description in the second column. The steps to calculate gust damage are explained more in detail as follows.

- Positive and negative acceleration fractions and their corresponding cumulative frequency of exceedance are read from the exceedance curve; Figure 4 shows the positive values of acceleration fraction (0.1 and 0.16) – see blue and red lines. Using these values, the respective cumulative frequency values are read (0.57 and 0.18) with the corresponding negative acceleration fraction at the same cumulative frequency level (-0.12 and -0.18).
- The difference between two successive values of cumulative frequency is used to calculate occurrence frequency. Occurrence frequency is the difference between two successive values of cumulative frequency. In this case, the difference between 0.57 and 0.18 results in 0.39 occurrences per nautical mile. The number of occurrences per hour is calculated by multiplying the cumulative frequency per nautical mile by the aircraft velocity in nautical miles per hour. For this example, the velocity was assumed as 148.2 nautical miles per hour (90% of the design velocity) resulting in 57.8 occurrences per hour.
- The stresses at this occurrence level (57.8) can be calculated by multiplying the acceleration fractions involved (0.13, the average between two successive positive values of 0.1 and 0.16, and -0.12) by the load limit factor (2.155) to obtain delta g. This delta g value is multiplied by the one-g stress value to obtain the maximum and minimum stress values.
- Using Eq. 2 and Eq. 3, the mean and alternating stresses are calculated and the life read from the relevant S-N curve (either deterministic or a realization from a probabilistic curve). Figure 5 [5] (AC23 - deterministic SN Curve) shows a deterministic example.

Table 2 shows the calculation summary for different acceleration fractions.

$$S_m = \frac{\left[(One - g\_stress) + pos\_delta\_g\right] + \left[(One - g\_stress) + neg\_delta\_g\right]}{2} \tag{2}$$

$$S_a = \left[(One - g\_stress) + pos\_delta\_g\right] - S_m \tag{3}$$

where S_m and S_a stand for mean stress and alternating stress that are needed to read the AC23 S-N curve.

- Having the mean and the alternating stresses and using Figure 5 [5] (Deterministic SN Curve), the life is calculated at each stress level. The lines in red in Figure 5 correspond to the values of mean and alternating stress used to calculate life for column 3 (first set of acceleration fractions) in Table 2.

Landing and Rebound Loads

Using the data presented in reference [5], an average value of 3.0 feet per second was established for the sink rate velocity. Reference [8] presents the results from landing gear drop test data, shown in Figure 6. With the sink rate velocity information, the load factor (g) can be calculated using linear regression as:

$$g = 0.1877 \cdot \left(\text{Sink Rate Velocity}\right) + 1.3422 \tag{5}$$

where 0.1877 is the slope and 1.3422 is the intercept. After calculating the load factor, the maximum and minimum stresses for landing and rebound are calculated using the equations:

$$Landing_{\max} = \frac{2}{3}\left(One - g\_Stress\right) \tag{6}$$

$$Landing_{\min} = \left(\text{ground\_Stress}\right)g \tag{7}$$

$$Rebound_{MAX} = 0.6 Landing_{MAX} \tag{8}$$

$$Rebound_{MIN} = 0.6 Landing_{MIN} \tag{9}$$

Finally, the alternating and mean stress values for landing and rebound can be calculated, the life read from Figure 5 and the damage determined.

Taxi Loads

The exceedance curve for taxi is shown in Figure 7 [5]. The damage for taxi is determined in an analogous manner to gust loading.

Ground-Air-Ground Loads

Ground-air-ground (GAG) is a cycle which is defined by the transition from the minimum ground stress to the maximum stress during a flight. A schematic for the ground-air-ground cycle is given in Figure 8.

The procedure to calculate the once-per-flight Peak-to-Peak GAG cycle is explained as follows:

- Using the gust and maneuver exceedances, determine the max stress per flight vs. the number of occurrences, see Figure 8.
- Add the number of occurrences in gust and number of occurrences in maneuver to obtain the total number of occurrences at each *max_GAG_stress* (shown as a green line in Figure 9).
- Load the maximum stresses for gust and maneuver including the corresponding number of occurrences per flight calculated from the exceedance curves.
- Interpolate the max stress to determine the *max_GAG_stress* which occur at a value of one occurrence per flight (shown as an orange line in Figure 9).
- *min_GAG_stress* is taken from landing, when the minimum stress occurs.
- Having the load pair, the life can be read from the S-N curve and the damage for the GAG cycle calculated.

Finally, the damage for the different stages is added and the damage per hour or per flight is calculated. Failure is assumed to occur when the Miner's coefficient reaches the critical value.

RANDOM VARIABLES

Given the significant airplane-to-airplane and flight-to-flight variations, an essential ingredient of the methodology is to investigate, develop, and model probability density functions (PDFs) of the critical input data, such as flight duration, aircraft speed, sink rate velocity, the

damage index coefficient and others. Probabilistic S-N curves were developed using data from an experimental program conducted by Wichita State University under a separate program [6, 7].

An overview of the random variables was presented in Table 1. Further details on the development of each random variable are given below.

Gust and Maneuver Loads

The gust and maneuver exceedance curves provide the information needed to compute the probability of obtaining various loading magnitudes. However, these exceedance curves themselves can vary. In order to create statistical distributions from the data contained in the NASA V-G/VGH database [11], Reyer [4] developed lognormal distributions for usages shown in Table 3. The distributions of usages for general aviation are used in the program. In each case, the best estimate for the coefficient of variation (COV) was 12%. As a result, the exceedance curve is a random variable.

Figure 10 shows random maneuver data schematically. The distributions are created at each acceleration level and the random data represents the frequency of occurrence. A realization of gust and maneuver exceedances is generated for each Monte Carlo sample. Figure 11 shows the confidence bounds for a random gust single-engine basic instruction usage.

Sink Rate

Exceedance information for sink rate velocity can be extracted from the Reference [5] and is presented graphically in Figure 12 in terms of cumulative frequency per 10,000 flights versus sink rate velocity. To generate samples from this exceedance curve, the data in Figure 12 is converted to a Cumulative Density Function (CDF) then samples are drawn using an inverse CDF method.

Flight Velocity-Duration

An example of flight velocity-duration statistical data that the user can input for any usage is shown in Table 4. The first two columns contain the flight duration information; the first column contains the flight time in hours, followed on the second column by the percentage of

flights that are flying with that time. The first row has the average speed during flight, expressed as percentage of the design velocity. The percentage of flights flown at that speed are inputted in each row. As many as one hundred and sixty-nine data points can be introduced in a 13 by 13 matrix.

Given the information in Table 4, the joint cumulative probability density function is created. To generate realizations, a pseudo random number is created and the flight time is read from its cumulative distribution function. Due to the fact that flight velocity and flight time are correlated, the same pseudo random number is used to generate flight velocity. An example of the joint probability density function is given in Figure 13.

Flight Weight-Duration

The same concept used for the flight duration-velocity matrix is utilized for the flight weight-duration matrix. The user inputs flight durations and weight percentages. These percentages will be used to generate random values for one-g stress and ground stress using the same process explained in the flight velocity and duration matrix. Table 5 shows an example of statistical data that the user can input for any usage. As many as one hundred and sixty-nine data points can be introduced in a 13 by 13 matrix.

Probabilistic Stress Life

Three different stress-life (SN) curves have been implemented. One is deterministic, called “AC23”, taken from Reference [5], see Figure 5. The two other curves correspond to probabilistic stress-life (P-S-N). To construct the P-S-N curves, constant amplitude fatigue test results developed experimentally under a research program by Wichita State University [6, 7] were used. The test data were developed for different coupon configurations at different maximum stress levels and mean stress. A summary of the data available for this study is shown in Table 6.

The two probabilistic methods implemented for the SN curves are explained as follows.

ASTM P-S-N

The ASTM P-S-N curves were constructed by fitting the test data employing "The Standard Practice for Statistical Analysis of Linear or Linearized Stress-Life (S-N) and Strain-Life (ε-N) Fatigue Data" (ASTM E739) [12]. This method assumes that the data is linear in logarithmic space and extrapolations outside the interval of the test data are not recommended. Run-outs or suspended tests are not included in the fitting. The following equation describes the relationship between stress and life:

$$\log N = A + B(\log S) \tag{14}$$

where: N is the life at the maximum value of constant amplitude cyclic stress S. The fatigue life N is the dependent (random) variable and the cyclic stress S is the independent (controlled) variable. It is assumed that the fatigue life is normally distributed, and the variance of the log of life is constant over the entire range of the independent variable S.

The maximum likelihood estimators of A and B can be calculated using the following equations:

$$\hat{B} = \frac{\sum_{i=1}^{k}(X_i - \overline{X})(Y_i - \overline{Y})}{\sum_{i=1}^{k}(X_i - \overline{X})^2} \tag{15}$$

$$\hat{A} = \overline{Y} + \hat{B}\overline{X} \tag{16}$$

where X represents $\log S$, Y represents $LogN$ and k denotes the number of data points and the overbar indicates the mean value.

The expression for estimating the variance is describes as follows:

$$\hat{\sigma}^2 = \frac{\sum_{i=1}^{k}(Y_i - \overline{Y}_i)^2}{k-2} \tag{17}$$

where $\overline{Y}_i = \hat{A} + \hat{B}\overline{X}_i$ and the $(k-2)$ term is used to make the variance an unbiased estimator.

For any simulation sampling, realizations of the ASTM P-S-N curves can be obtained by sampling from the equation

$$\hat{Y}_r(X) = \hat{A} + \hat{B}X \pm \sqrt{2F_{\nu_1,\nu_2}}\hat{\sigma}\left[\frac{1}{k} + \frac{\left(X-\overline{X}\right)^2}{\sum_{i=1}^{k}\left(X_i-\overline{X}\right)^2}\right]^{\frac{1}{2}} \tag{18}$$

where F_{ν_1,ν_2} denotes the F-distribution with ν_1 and ν_2. The degrees of freedom calculated as: $\nu_1 = l-2$ and $\nu_2 = k-l$, k represents the number of tested data points, l represents the different number of stress levels. A Bernoulli distribution is used to randomly sample the "$\pm$" sign in Eq. 18.

The test for linearity based on the ASTM standard is based on the F_{ν_1,ν_2} distribution using the following equation:

$$F_{Test} = \frac{\sum_{i=1}^{l} m_i\left(\hat{Y}_i - \overline{Y}_i\right)^2/(l-2)}{\sum_{i=1}^{l}\sum_{j=1}^{m_i} m_i\left(Y_{ij} - \overline{Y}_i\right)^2/(l-1)} \tag{19}$$

where l stands for the different number of stress levels of X ($\log S$) and m_i is the number of replicate values of Y ($LogN$) at each X_i ($\log S_i$). The hypothesis of linearity is rejected when the computed value in Eq. 19 exceeds F_{ν_1,ν_2} distribution. The test calculates the ratio of the predicted values against the tested results. If the linearity test (F_{test}) exceeds the F_{ν_1,ν_2} value at the desire confidence level the hypothesis is rejected. When the linearity test is rejected it is recommended that a nonlinear polynomial model be considered, as described in the following section.

For the ASTM method, the 95% confidence bounds are calculated using Eq. 18 at each stress test level. The F_{ν_1,ν_2} value is calculated at a cumulative probability of 0.95 with the two degrees of freedom (ν_1,ν_2) as explained above. Some linearity test results are shown in Table 7 at 5% significant level. It is clear that for the cases presented in this table it is recommended a nonlinear model like the polynomial model.

Two different ASTM P-S-N curve results are shown in semi-log space in Figure 14 and Figure 15. Each figure shows the mean value with a solid line, the 95 percent confidence bounds with dashed lines, and the test data [6, 7] are shown as blue triangles.

Polynomial P-S-N

A more flexible method for fitting the S-N data was developed by implementing a polynomial equation in log-log space up to a fourth order. Lower orders can be fit if the data does not require the higher orders. The polynomial P-S-N curves were constructed by fitting the test data from References [6, 7] and excluding run outs. The fourth order polynomial equation is,

$$\log(N) = b + A\left(S_{center}\right) + B\left(S_{center}\right)^2 + C\left(S_{center}\right)^3 + D\left(S_{center}\right)^4 \tag{20}$$

where b represents the intercept from the regression and $S_{center} = \log(S) - \frac{1}{n}\sum_{i=1}^{n}\log(S_i)$, that is, S_{center} is a "centered" stress in log space after subtracting the mean of $\log(S)$. Using a centered stress improved residual values improving the polynomial fits.

Realizations of the polynomial P-S-N curves are generated using the residual data with the assumption that the residuals (e) will follow a normal distribution with mean zero and constant standard deviation ($e \sim Normal(0,\sigma)$). To generate samples using residual information the following equation is used.

$$\log(N) = b + A\left(S_{center}\right) + B\left(S_{center}\right)^2 + C\left(S_{center}\right)^3 + D\left(S_{center}\right)^4 + \left(Z\sigma_e\right) \tag{21}$$

where σ_e is the residual standard deviation and $Z \sim N(0,1)$.

The 95% confidence bounds for the polynomial are calculated using Eq. 21 at each stress levels. For the standard normal variable (Z) a value equal to 1.96 is used which corresponds to the 0.95 cumulative probability value for the standard normal distribution.

Two different polynomial P-S-N curve results are shown in Figure 16 and Figure 17. Each figure shows the mean value with a solid line, the 95 percent confidence bounds with dashed lines, and the test data [6, 7] are shown using blue triangles.

Stress Severity Factor

The stress severity factor (SSF) [13] is a fatigue quality number that emphasizes the fatigue characteristics of the structure rather than its static strength.

The SSF is defined by the following equation.

$$SSF = \frac{\alpha \cdot \beta}{S}\left(K_{tb} \times \theta \times \frac{\Delta P}{d \cdot t} + K_{tg} \times \frac{P}{w \cdot t}\right) \tag{22}$$

where K_{tg} is the stress concentration factor for the gross area, K_{tb} is the stress concentration factor for the bearing stress, P is the bypassing load, ΔP is the load transfer through the fastener, α accounts for the hole quality, β is the hole filling factor that accounts for the interference between the fastener and the hole, θ is the bearing distribution factor that accounts for the effect of non-uniformity of bearing stress on the hole surface, w is the width of the specimen, t is the thickness of the specimen, and d is the diameter of the fastener (see Figure 18).

The different parameters of the SSF can be developed for different specimens where the amount of transferred load and bypass load is known. The hole quality value α is 1.0 for standard holes and 0.9 for drilled and reamed holes. The SSF can be written as a function of the unknown parameters, β and θ, by identifying the ratios of fatigue strengths of different specimens with the inverse ratios of their SSF numbers [13].

The β parameter is developed using the tested open hole (OH) data and the tested filled hole (FH) data. In order to determine the parameter, SMART|LD uses the fact that the OH and FH fatigue strengths are inversely proportional to their SSF values as shown in Eq. 23 and in Figure 19.

$$\frac{S\left(N_f\right)_{OH}}{S\left(N_f\right)_{FH}} = \frac{SSF_{FH}}{SSF_{OH}} \tag{23}$$

To generate β as a function of life, the methodology sweeps through the life values and reads the stress values $S(N_f)$ for the OH and FH configurations at that specific life. Then, assuming by definition $\beta_{OH} = 1,\ \alpha_{OH} = 1,\ \alpha_{FH} = 1$, and that for FH and OH the load transfer is zero, β_{FH} can be computed using Eq. 25 developed from Eq. 24. K_{tg} values cancel out because the geometry of both coupons is the same.

$$\frac{S(N_f)_{OH}}{S(N_f)_{FH}} = \frac{\alpha_{FH} \cdot \beta_{FH} \cdot K_{tg}}{\alpha_{OH} \cdot \beta_{OH} \cdot K_{tg}} \tag{24}$$

The results indicate that

$$\beta_{FH}(N_f) = \frac{\alpha_{OH} \cdot \beta_{OH} \cdot S(N_f)_{OH}}{\alpha_{FH} \cdot S(N_f)_{FH}} \tag{25}$$

where S denotes the far field stress.

Having the values for β, the values for the θ for the different load transfer configurations can be computed using Eq. 27. β_{FH} in this equation can be calculated using Eq. 25. α_{OH} and α_{FH} are assumed equal. The stress concentration factor for the gross area (K_{tg}) and the stress concentration factor for the bearing stress (K_{tb}) can be found in reference 14.

$$\frac{S(N_f)_{OH}}{S(N_f)_{FH}} = \frac{\alpha_{FH} \cdot \beta_{FH} \left\{ K_{tb} \cdot \theta \cdot LT \cdot \frac{w}{d} + K_{tb}(1 - LT) \right\}}{\alpha_{OH} \cdot \beta_{OH} \cdot K_{tg}} \tag{26}$$

Rearranging, the equation for θ yields

$$\theta = \frac{\frac{S(N_f)_{OH} \cdot \beta_{OH} \cdot K_{tg}}{S(N_f)_{FH} \cdot \beta_{FH}} - K_{tb}(1 - LT)}{K_{tg} \cdot LT \cdot w/d} \tag{27}$$

Finally, having β and θ, the SSF as a function of the far field stress can be calculated from the following equation developed from Eq. 22:

$$SSF = \alpha\beta \left(K_{tb} \times \theta \times LT \times \frac{w}{d} + K_{tg}(1 - LT) \right) \tag{28}$$

where $LT = \Delta P / P$.

Using Eq. 23, the SSF can be used to predict different S-N curves. For example, given the S-N data for OH (SSF = 3), the life for SSF = 2.6 can be calculated as follows. Eq. 23 can be rewritten as:

$$\frac{S_{\max}(N_f)^{@\ \mathrm{SSF_{Any}}}}{S_{\max}(N_f)^{@\ \mathrm{SSF_{OH}}}} = \frac{SSF_{OH}}{\mathrm{SSF_{Any}}} \tag{29}$$

and the SSF Ratio is calculated as

$$\text{SSF Ratio} = \frac{SSF_{OH}}{\mathrm{SSF_{Any}}} = \frac{3}{2.6} = 1.15 \tag{30}$$

With this SSF Ratio, the S-N curve for SSF = 2.6 can be calculated as shown in Eq. 31 and Figure 20.

$$S_{\max}{}^{@\ \mathrm{SSF_{Any}}} = (\text{SSF Ratio}) \cdot S_{\max}{}^{@\ \mathrm{SSF\ OH}} \tag{31}$$

Miner's damage index

Miner's rule dictates that failure occurs when the damage index (D) exceeds one [14]. However, numerous comparisons with test results show that failure occurs for a range of damage index values and the results are case and material dependent. As a result, the methodology developed here can be used to determine a probability distribution for the damage index given the variable amplitude loading and the P-S-N curves from constant amplitude loading. This distribution can then be input for future analyses to determine the flights or hours-to-failure.

The methodology employed to generate the damage index probability distribution is shown schematically in Figure 21 and explained as follows:

- Representative variable amplitude stress spectrums for different aircraft usages (special, normal and aerobatic) and stress levels (low, medium, and high) are generated.
- Utilizing the appropriate stress severity factor from the test article, the same variable amplitude spectrum used during testing, and the P-S-N curves developed from constant amplitude tests, the number of flights to failure from the test article is simulated in the software and the damage index at failure recorded. This process is repeated using Monte Carlo sampling of the P-S-N curve for this test to assess the effects of a variable S-N curve.
- This procedure is repeated for each test article and the ensemble of data used to develop the probability distribution of the damage index. The procedure is shown in Figure 21.

RISK OUTPUTS

A number of probabilistic outputs can be used to develop an understanding of the analysis results. In particular, the cumulative distribution function and probability density function of flights-to-failure, hours-to-failure, the hazard function, Pearson correlation coefficient, histograms and scatter plots are all useful quantities. Design scans can be developed in order to quickly assess the effects of deterministic parameters. These capabilities are summarized as follows:

Probability of Failure (POF)

The probability-of-failure is calculated using the "damage" mode described above. The damage is accumulated as a function of the number of hours until the accumulated damage equals or exceeds Miner's damage index. When the damage recorded is larger than the random Miner's damage coefficient generated for that sample, a failure is counted. The process is repeated for each Monte Carlo sample. When the Monte-Carlo sampling is complete, the total number of failures is divided by the number of samples. Finally the 90, 95 and 99 percent confident bounds from the of the POF are calculated.

Hazard function

The hazard function is used to calculate the risk of failure in the next increment of hours conditioned on no failures before that time. The hazard function is calculated using Eq. 32.

$$hz(t) = \frac{PDF(t)}{1 - CDF(t)} \tag{32}$$

Correlation Coefficients

Pearson correlation coefficients are computed to indicate the relative importance of the random variables. A high correlation coefficient indicates that a variable is important. The Pearson coefficient is calculated using the following equation,

$$\rho_{x,y} = corr(X,Y) = \frac{\sum_{i=1}^{n}\left(X_i - \overline{X}\right)\left(Y_i - \overline{Y}\right)}{\sqrt{\sum_{i=1}^{n}\left(X_i - \overline{X}\right)^2}\sqrt{\sum_{i=1}^{n}\left(Y_i - \overline{Y}\right)^2}} \tag{33}$$

CASES STUDIES

Two different case studies application are presented to demonstrate the methodology. The first case considers a high performance single-engine airplane with 4,000 pounds of maximum take off weight analyzed using a single usage (Single Engine Unpressurized Executive Usage). The airplane and flight characteristics are presented in Table 8. For this first case study all the three different S-N curves available in this work were used. A total 20,000 samples were run and the safe-life of the airplane calculated.

The safe life calculated as a function of the hours to failure is shown in Table 9 for the three different S-N curves.

Using goodness-of-fit tests, the hours-to-failure distribution closely follows a lognormal distribution. The probability density function of hours-to-failure is shown in Figure 23.

Sensitivity analysis with respect to flights-to-failure using Pearson correlation coefficients is shown in Table 10. The results indicate the high importance of multiple factors: damage index, gust and maneuver factors, one-g stress, ground stress and the P-S-N curve (AC23 is a deterministic SN curve so there is no samples to calculate Pearson coefficient).

Three different scatter plots with respect to hours-to-failure are presented in Figure 24, Figure 25 and Figure 26. The scatter plots include a histogram of each of the random variables used to create the scatter plot.

For this specific usage, probability values from the cumulative distribution of the safe life hours to failure are shown in Table 11.

Figure 27 shows the hazard function of hours-to-failure based on the three different PSN curves. The results indicate an almost linear increase in risk with respect to flight hours assuming no previous failure for all three. Polynomial PSN is the most conservative for this specific case. This behavior can be explained because the stress levels contained on each flight spectrum for this case lay between 8 KSI and 17 KSI mostly as shown in Figure 28. Figure 29 shows the regions where polynomial P-S-N curve is more conservative compared with the ASTM P-S-N curve. The stresses for each of the flight spectrum are contained on this conservative region making the polynomial analysis more conservative.

Figure 28 presents a histogram showing the P-S-N region percentage damage. The height of each column describes the percentage of damage within each region of the P-S-N curve.

The second case study, a twin engine airplane with 36000 pounds of maximum take off weight considered in mix usage (Twin Engine General Usage and Twin Engine Instructional Usage) was analyzed in hours mode. The hours methodology allows the user to specify a number of flying hours for each usage, this case study was conducted to calculate the probability-of-failure if the aircraft is flown for 10,000 hours in General usage (current condition), and then flown for another 1,000, 2,000, 3,000, and 4,000 additional hours under the Instructional usage. The main advantage of this analysis is to have estimate of the risk (probability-of-failure) of an airplane flying any number of additional hours from its current condition. The airplane and flight characteristics are presented in Table 12.

First the safe-life of the aircraft using the General usage was calculated to have an estimated of the time to crack initiation on this airplane. Table 13 shows the safe-life results.

Figure 30 and Figure 31 shows scatter plots with respect to the normalized cumulated damage. In this figure the red dots represent Instructional usage and blue dots represent General usage. The Y-axis is the normalized cumulated damage. From the qualitative analysis it is clear that the red dots are concentrated more heavily towards the low normalized cumulated damage than the blue dots. Hence one can conclude that Instructional usage is more severe than general usage.

Figure 32 shows the normalized cumulative damage and Probability-of-Failure for each of the five different scenarios. The results show an increment on the cumulated damage and on the probability of failure. It can be observed that twin-engine instructional usage is more severe than twin-engine general usage; this behavior can be explained because amount of accumulated damage and the increment in the probability of failure were doubled after the 4,000 additional hours in instructional usage.

CONCLUSIONS

Probabilistic fatigue evaluation of General Aviation aircraft is vital in order to provide insight into the severity or criticality of a potential structural issue. For this reason, a probabilistic risk assessment methodology and computer software were developed such that FAA engineers can perform a risk assessment of a structural issue. Due to significant airplane-to-airplane and flight-to-flight variations, probability density functions of the critical variables were investigated and developed.

The methodology was programmed into a computer code, "SMART|LD" to quantify the risk assessment and risk management of GA structural issues. This information will provide a proactive approach to enable a nonbiased review of data to assure airworthiness. The software considers the random variables: loading (Gust and Maneuver Loads, Sink Rate, Flight Velocity-Duration, Flight Weight-Duration), S-N material behavior (Probabilistic Stress-Life (P-S-N) curves developed from constant amplitude tests), the Stress Severity Factor, and Miner's damage index. The random variables are used inside a Monte Carlo simulation to calculate the airplane safe-life, probability-of-failure, and sensitivity analysis based upon a Miner's linear damage rule.

Program outputs include the cumulative distribution function and probability density function of hours-to-failure, the hazard function, and scatter plots. Design scans can be developed in order to quickly assess the effects of deterministic parameters. Correlation coefficients are computed to indicate the relative importance of the random variables. The methodology and software were demonstrated on two applications to a structural risk assessment.

Two case studies were run to demonstrate the methodology and its applicability to different scenarios. Those scenarios includes to calculate the airplane safe-life or to assess the risk of an airplane based on the current condition and its predicted usage.

The results indicate the high importance of multiple factors: damage index, gust and maneuver factors, one-g stress, ground stress, and the P-S-N curve. For low stress levels (below 15 KSI) and high stress levels (above 32 KSI) polynomial P-S-N is more conservative in terms of flights-to-failure, hours-to-failure, and the hazard function when it compares to the ASTM P-S-N curve. For high stresses levels ASTM P-S-N curves should be used with caution because predicted values might be showing lives longer that the tested values.

ACKNOWLEDGEMENTS

This work was accomplished under a Federal Aviation Administration grant 07-G-011, Dr. Felix Abali program manager. The authors would like to acknowledge Dr. Felix Abali, Dr. Michael Shiao, Marv Nuss, Michael Reyer, and Dr. Herb Smith for providing insightful discussions throughout the completion of this project.

REFERENCES

1. Miedlar, P.C., Berens, A.P., Hovey, P.W., Boehnlein, T.R. and Loomis, J.S., "PRoF v3 PRobability Of Fracture," University of Dayton Research Institute, USAF Contract Number F09650-03-D-0001, December 2005
2. J.W. Lincoln, "Risk Assessment of an Aging Military Aircraft," J. Aircraft, 22, 8, August 1985, 687-691
3. G.R. Leverant, H.R. Millwater, R.C. McClung, M.P. Enright, "A New Tool for Design and Certification of Aircraft Turbine Rotors," Journal of Engineering for Gas Turbines and Power, Vol. 126, No. 1, pp. 155-159, 2004
4. Reyer W.M., "Probability Basis of Safe-Life Evaluation in Small Airplanes." Aging Aircraft Conference. Atlanta, March 2006.
5. FAA AC 23-13A, "Fatigue Fail-Safe, and Damage Tolerance Evaluation of Metallic Structure for Normal, Utility, Acrobatic, and Commuter Category Airplanes." 2005.
6. Raju, K.S., Smith, K.S., Caido, F., Gomez, C., Shiao, M., "Fatigue Behavior of Fastener Joints." SAE International Journal of Aerospace, Vol. 1 No.1, 2009, pp 675-684
7. Raju, K.S., Smith, B. L., Caido, F., Gomez, C., Shiao, M., Nuss, M., "Fatigue-Based Severity Factors for Shear-Loaded Fasteners." AIAA Journal of Aircraft, Vol. 47, No. 1, 2010, pp 181-191.
8. FAA AFS120-73-2, "Fatigue Evaluation of Wing and Associated Structure on Small Airplanes." 1973.
9. Ocampo, J.D., Acosta, C.A., Millwater, H., "High Performance Computing Implementation on a Risk Assessment Problem." 48th AIAA Aerospace Sciences Meeting, Orlando, FL, January 2010.
10. Singh, G., Acosta, C.A., Ocampo, J., Millwater, H., "Distributed Computing for Probabilistic Structural Integrity Analysis of Aircraft Structures," 51st AIAA/ASME/ASCE/AHS/ASC Structures, Structural Dynamics, and Materials Conference Orlando, FL, April 2010.
11. DOT/FAA/CT-91/20 "General Aviation Aircraft—Normal Acceleration Data Analysis and Collection Project." 1993.
12. ASTM E739-91 (Reapproved1998), Statistical Analysis of Linear or Linearized Stress-Life (S-N) and Strain-Life (e-N) Fatigue Data (1998).

13. Jarfall, L., “Optimum design of joints: the stress severity factor concept, Aircraft Fatigue, Design, Operational and Economic Aspects.” Pergamon, Australia, J.Y. Mann and I.S. Milligan Eds., 1972, pp. 337-380.
14. Niu, C.Y., “Airframe Structural Design.” Granada Hills, CA: ADASO/ADASTRA Engineering Center. 2006.
15. Miner M. A., “Cumulative Damage in Fatigue.” Journal of Applied Mechanics, 1945, pp. A159-A164.

TABLES

Table 1. Code Variable Classification

Variable	Type
Gust/Maneuver Load Exceedances	Probabilistic (Lognormal) [4]
Aircraft Velocity and Flight Duration	Probabilistic (joint PDF)
Sink Rate	Probabilistic [5]
Ground Stress and One-g Stress	Probabilistic (joint PDF, user defined)
Maneuver Load Limit Factors	Deterministic (aircraft specific)
Gust Load Limit Factors	Deterministic (aircraft specific)
P-S-N	Probabilistic (determined from regression modeling of constant amplitude tests) [6,7]
Stress Severity Factor	Probabilistic (Developed from P-S-N Curves)
Miner's Damage Index	Probabilistic (Weibull or Normal – fit to variable amplitude tests) [6,7]

Table 2 Gust Damage Calculation

Gust Damage					
1	From the exceedance curve reading the positive values of the gust load factor ratio a_n / a_{nLLF}	0.10	0.16	0.22	0.28
		0.16	0.22	0.28	0.34
2	Calculate the average value from the values in Row 1	0.13	0.19	0.25	0.31
3	From Figure 4 read the different values of cumulative occurrence of gust per nautical mile at a specific gust load factor.	0.57	0.18	0.052	0.013
4	From the exceedance curve, read the negative values of the gust load factor ratio corresponding to Row 2.	-0.12	-0.18	-0.25	-0.32
5	Frequency per nautical mile (no accumulation) is the difference between two successive values in Row 3.	0.39	0.128	0.039	0.0087
6	Number of gust cycles accumulated per hour (Row 5) x 0.9(Design Cruise Speed,Vc).	57.8	19	5.79	1.292
7	Increment in the stress due to the gusts. To get this value (delta g) multiply Row 2 and Row4 by $a_{nLLF} = 2.155$	-0.259	-0.388	-0.539	-0.690
		0.28	0.409	0.539	0.667
8	Maximum and minimum delta stress over and below the maximum stress at the critical component (One-g Stress) – multiply Row (7) by One-g Stress (7410 psi)	-1920	-2870	-4000	-5980
		2070	3030	4000	4940
9	Mean stress (psi). This is calculated as in Eq. 2.	7485	7490	7410	7325
10	Alternating stress (psi) calculation. This is calculated as in Eq. 3.	1995	2950	4000	5025
11	Endurance cycles, N, read from Figure 5 is (S-N diagram) $x10^6$.	14	3.1	1.05	0.50
12	Damage per hour, Row (6) divided by row (10) $x10^{-6}$	4.13	6.13	5.52	2.59

Table 3. Probabilistic Usage Groups

Usage Group
Single-Engine Unpressurized Usage Basic Flight Instruction
Single-Engine Unpressurized Usage Personal Usage
Single-Engine Unpressurized Usage Executive Usage
Single-Engine Unpressurized Usage Aerobatic Usage
Twin-Engine Unpressurized Usage Basic Flight Instruction
Twin-Engine Unpressurized Usage General
Pressurized Usage
Agricultural Usage

Table 4. Flight Length and Airspeed Data

		Average Speed During Flight, % Design Velocity						
Flight time (Hours)	**% of Flights**	1.00	0.95	0.90	0.85	0.80	0.75	0.70
0.25	0	0.0	0.0	0.0	0.0	0.0	0.0	0.0
0.50	0.05	0.0	0.0	0.05	0.25	0.6	0.1	0.0
0.75	0.15	0.0	0.0	0.25	0.4	0.3	0.05	0.0
1.00	0.35	0.05	0.15	0.45	0.3	0.05	0.0	0.0
1.25	0.1	0.05	0.15	0.45	0.3	0.05	0.0	0.0
1.50	0.1	0.05	0.3	0.5	0.15	0.0	0.0	0.0
1.75	0.2	0.05	0.3	0.5	0.15	0.0	0.0	0.0
2.00	0.05	0.15	0.55	0.2	0.1	0.0	0.0	0.0

Table 5. Flight Length and Weight Data

		Weight (one-g stress and Ground stress) Percentage						
Flight time (Hours)	**% of Flights**	1.00	0.95	0.90	0.85	0.80	0.75	0.70
1.00	0.35	0.05	0.15	0.45	0.3	0.05	0.0	0.0
1.25	0.1	0.05	0.15	0.45	0.3	0.05	0.0	0.0
1.50	0.1	0.05	0.3	0.5	0.15	0.0	0.0	0.0
1.75	0.2	0.05	0.3	0.5	0.15	0.0	0.0	0.0
2.00	0.05	0.15	0.55	0.2	0.1	0.0	0.0	0.0

Table 6. Data Available to Develop P-S-N Curves [6,7]

Coupon Configuration	Maximum Stress [KSI]	Number of Data Points	Mean Stress [KSI]
Open Hole	42, 32, 18, 12, 10, and 9.25	39	3
Open Hole	42, 32, 20, 18, 15, 12.5, and 11.5	37	6
Hilok Filled Hole	42, 32, 24, 18, and 14	32	3
Hilok Filled Hole	42, 32, 30, 24, 21 and 16	36	6
Hilok 30 % Load Transfer	42, 32, 24, 15, and 8	34	3
Hilok 30 % Load Transfer	42, 32, 24, 15, and 11	36	6
Hilok 50 % Load Transfer	42, 32, 24, 15, and 8	36	3
Hilok 50 % Load Transfer	42, 32, 24, 15, and 11	43	6
Rivet Filled Hole	46, 42, 32, 30, 21, 17.5, and 14	42	3
Rivet Filled Hole	48, 44, 32, 30, 21, 18, and 16	43	6
Rivet 50 % Load Transfer	42, 32, 28, 20, and 13	34	3
Rivet 50 % Load Transfer	42, 32, 28, 20, and 13	30	6

Table 7. ASTM Linearity Test

Coupon Configuration	$F_{\nu_1,\nu_2}(5\%)$	F_{Test}
Open Hole 6 KSI	2.53	23.87
Hilok 50% Load Transfer 6 KSI	2.86	3.11
Rivet 50% Load Transfer 3 KSI	2.94	9.61

Table 8. Input Data for Case Study One

Case Study One	
Variable	**Value**
Usage	Single Engine Unpressurized Executive Usage
Design LLF Maneuver	3.41, -1.41
Design LLF Gust	3.80, -1.52
Ground Stress (psi)	-2,000
One-g stress (psi)	6,550
Flight length and Velocity Matrix	Dur/Vel 0.80 0.85 0.90 0.95 1.00 0.50: 0.05 0.05 0.10 0.10 0.10 0.65 0.60: 0.05 0.05 0.05 0.05 0.15 0.70 0.70: 0.10 0.00 0.05 0.05 0.15 0.75 0.80: 0.15 0.00 0.05 0.05 0.10 0.80 0.90: 0.20 0.00 0.00 0.00 0.10 0.90 1.00: 0.25 0.00 0.00 0.05 0.05 0.90 1.10: 0.15 0.00 0.00 0.00 0.05 0.95 1.20: 0.05 0.00 0.00 0.00 0.05 0.95
Flight length and Weight Matrix	Dur/Wei 0.80 0.85 0.90 0.95 1.00 0.50: 0.05 0.00 0.00 0.00 0.20 0.80 0.60: 0.05 0.00 0.00 0.00 0.20 0.80 0.70: 0.10 0.00 0.00 0.00 0.15 0.85 0.80: 0.15 0.00 0.00 0.00 0.15 0.85 0.90: 0.20 0.00 0.00 0.00 0.10 0.90 1.00: 0.25 0.00 0.00 0.00 0.10 0.90 1.10: 0.15 0.00 0.00 0.00 0.05 0.95 1.20: 0.05 0.00 0.00 0.00 0.05 0.95
Average Velocity (Vno/Vmo(Knots)	153
Miner's Rule Damage Factor	Normal 1.0 (μ) 0.1(σ)
MCSAMP	20,000
SN Curve	AC23, ASTM, and Polynomial
Analysis Type	Damage

Table 9. Safe-life Analysis Results Case Study One

	95% Confidence Bound	Mean	95% Confidence Bound
AC-23	41,109	41,277	41,445
ASTM	46,043	46,227	46,043
Polynomial	72,997	73,557	74,118
	95% Confidence Bound	**Standard Deviation**	**95% Confidence Bound**
AC-23	11,998	12,116	12,236
ASTM	13,180	13,309	13,441
Polynomial	40,073	40,466	40,866

Table 10. Pearson Coefficient Results.

	Flights Duration	Flight Speed	Sink Rate	Damage Coefficient	Gust Factor	Maneuver Factor	One-g Stress	Ground Stress	PSN
AC23	0.07	-0.06	-0.02	0.34	0.86	0.07	-0.30	0.30	0.00
ASTM	0.00	-0.10	-0.01	0.35	0.66	0.07	-0.28	0.28	0.41
POLY	-0.03	-0.06	-0.03	0.18	0.69	0.05	-0.45	0.45	0.35

Table 11. CDF of Hours-to-Failure

Probability	Hours to Failure AC23	Hours to Failure ASTM	Hours to Failure Polynomial
0.500	40,445	44,343	65,114
0.100	26,462	30,332	33,120
0.010	16,314	21,533	17,519
0.001	10,280	16,391	10,057
0.000223	7,247	12,698	6,178

Table 12. Input Data for Case Study Two

Case Study Two							
Variable	**Value**						
Usage 1	Twin Engine Unpressurized General Usage						
Design LLF Maneuver	2.77, -1.0						
Design LLF Gust	2.70, -0.77						
Ground Stress (psi)	-7000						
One-g stress (psi)	7700						
Flight length and Velocity Matrix	Dur/Vel		0.75	0.80	0.85	0.90	0.95	1.00
	0.50:	0.45	0.05	0.30	0.50	0.10	0.05	0.00
	0.75:	0.40	0.00	0.20	0.30	0.35	0.10	0.05
	1.00:	0.10	0.00	0.05	0.30	0.45	0.15	0.05
	1.25:	0.05	0.00	0.05	0.20	0.25	0.20	0.30
Flight length and Weight Matrix	Dur/Wei		0.75	0.80	0.85	0.90	0.95	1.00
	0.50:	0.45	0.05	0.30	0.50	0.10	0.05	0.00
	0.75:	0.40	0.00	0.20	0.30	0.35	0.10	0.05
	1.00:	0.10	0.00	0.05	0.30	0.45	0.15	0.05
	1.25:	0.05	0.00	0.05	0.20	0.25	0.20	0.30
Average Velocity (Vno/Vmo(Knots)	185						
Usage 2	Twin Engine Unpressurized Basic Instructional Usage						
Design LLF Maneuver	2.77, -1.0						
Design LLF Gust	2.70, -0.77						
Ground Stress (psi)	-7000						
One-g stress (psi)	7700						
Flight length and Velocity Matrix	Dur/Vel		0.75	0.80	0.85	0.90	0.95	1.00
	0.50:	0.50	0.05	0.30	0.50	0.10	0.05	0.00
	0.75:	0.40	0.00	0.20	0.30	0.35	0.10	0.05
	1.00:	0.10	0.00	0.05	0.30	0.45	0.15	0.05
Flight length and Weight Matrix	Dur/Wei		0.75	0.80	0.85	0.90	0.95	1.00
	0.50:	0.50	0.05	0.30	0.50	0.10	0.05	0.00
	0.75:	0.40	0.00	0.20	0.30	0.35	0.10	0.05
	1.00:	0.10	0.00	0.05	0.30	0.45	0.15	0.05
Average Velocity (Vno/Vmo(Knots)	185						
Miner's Rule Damage Factor	Normal 1.0 (μ) 0.1(σ)						
MCSAMP	20,000						
SN Curve	ASTM						
Analysis Type	Hours						

Table 13. Safe-life Analysis Results Case Study Two.

Hours-to-Failure		
95% Confidence Bound	**Mean**	**95% Confidence Bound**
25,635	25,951	26,266
Hours-to-Failure ASTM		
95% Confidence Bound	**Mean**	**95% Confidence Bounds**
15,864	16,084	16,310

FIGURES

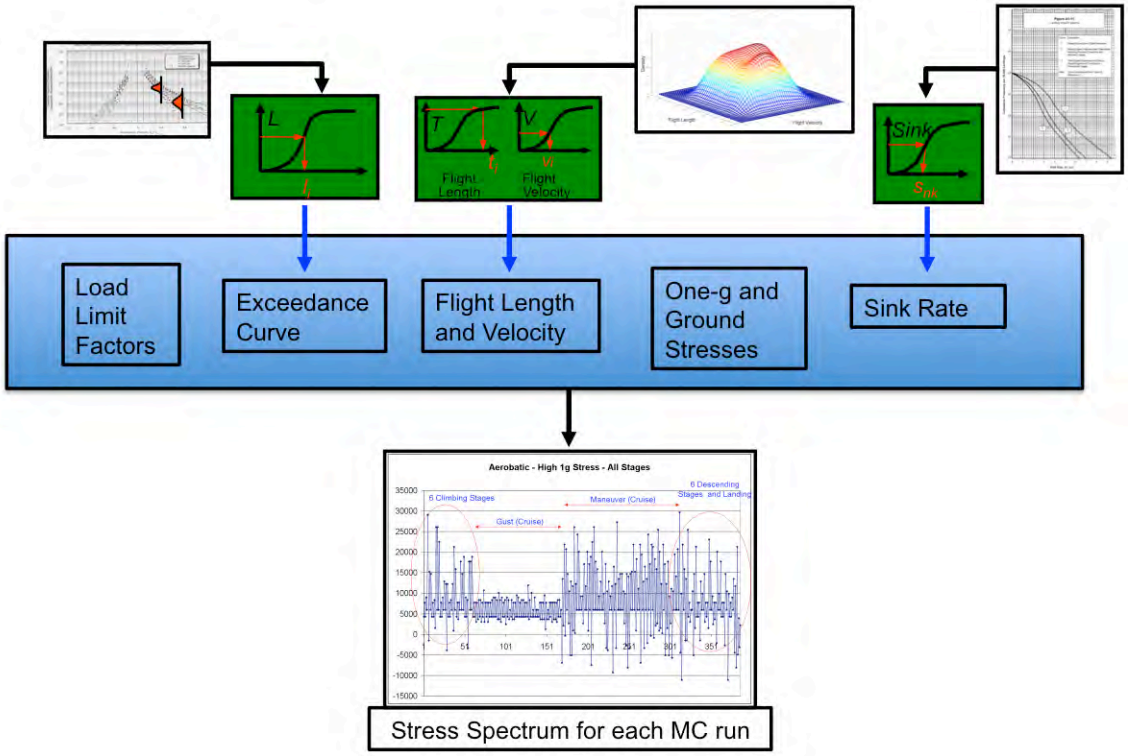

Figure 1. Schematic of Risk Assessment Methodology for the Spectrum Generation

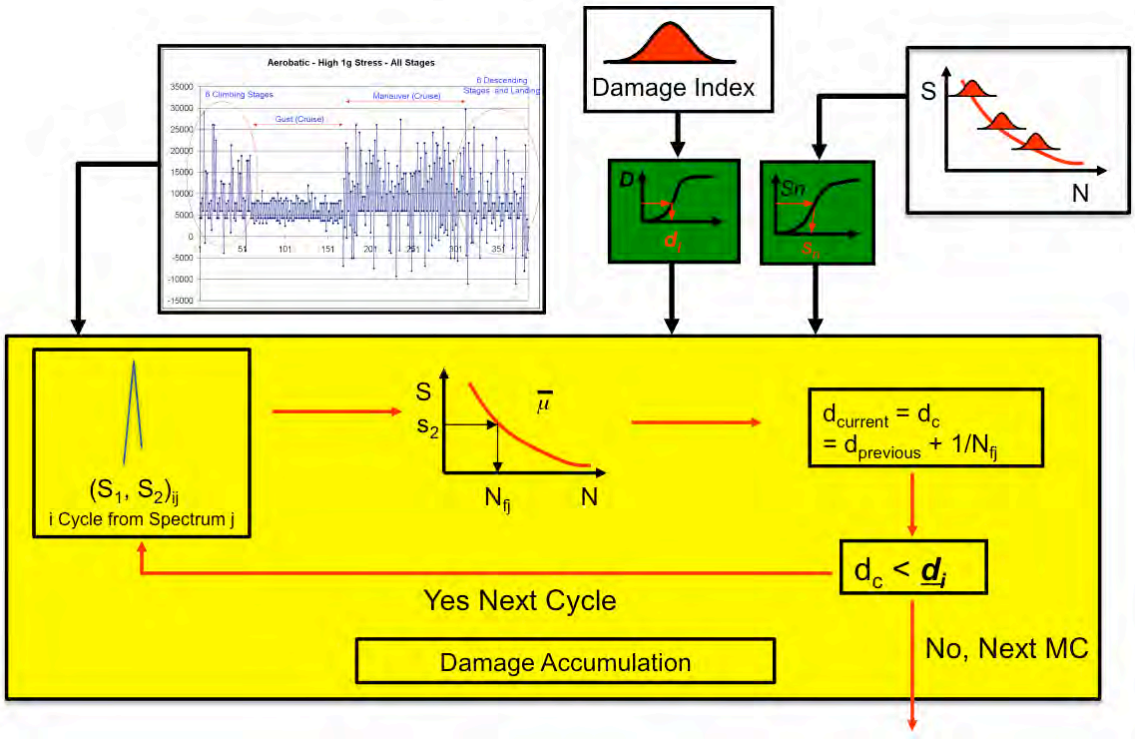

Figure 2. Schematic of Risk Assessment Methodology for the Damage Accumulation

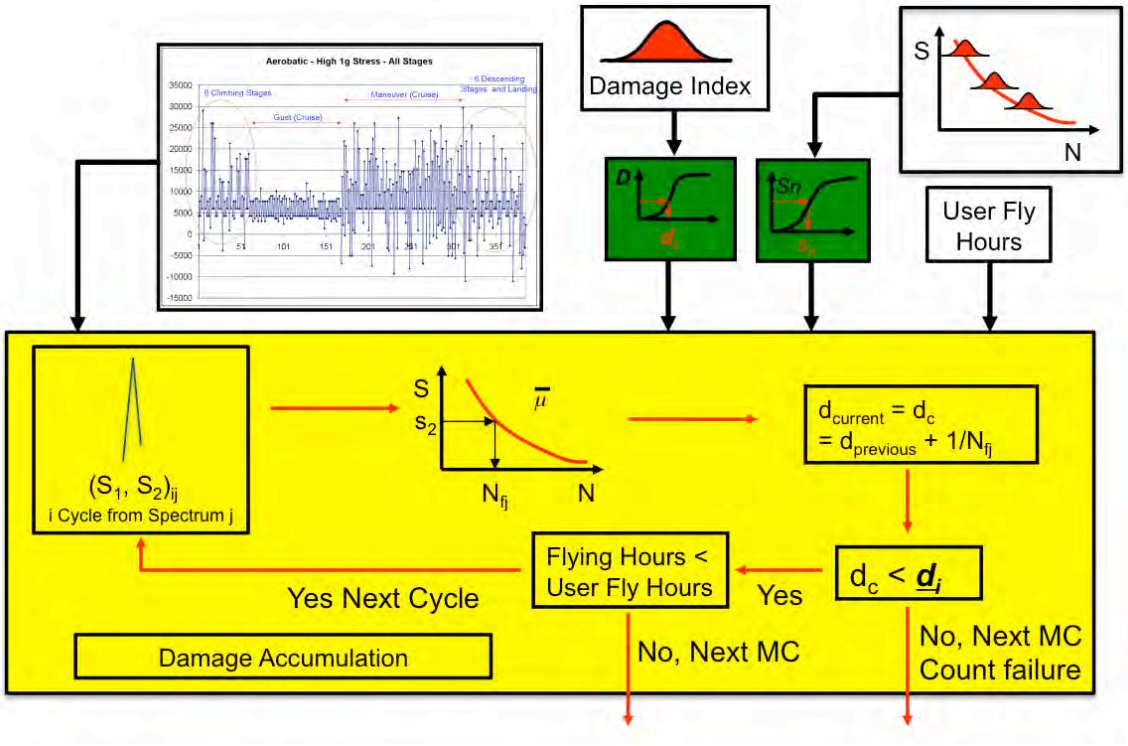

Figure 3. Schematic of Risk Assessment Methodology for Damage Accumulation

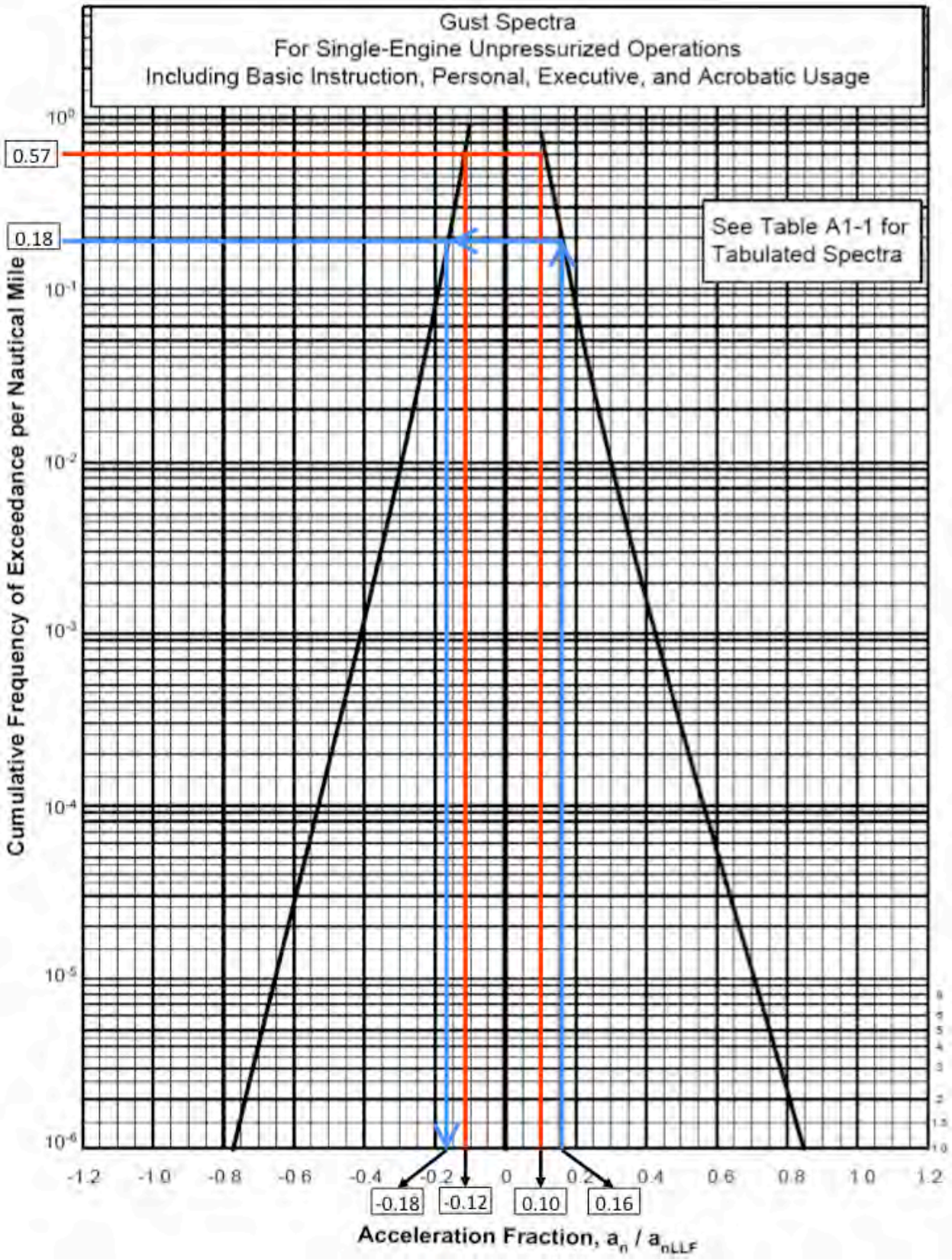

Figure 4 Exceedance Curve for Gust

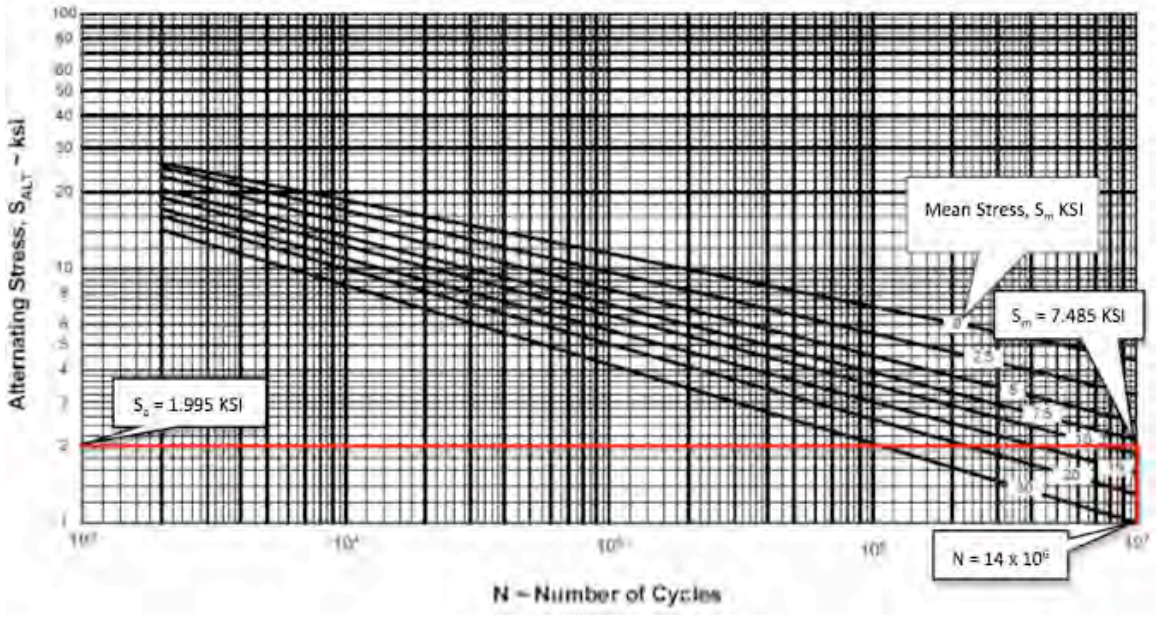

Figure 5 S/N Curves for Aluminum Components [5]

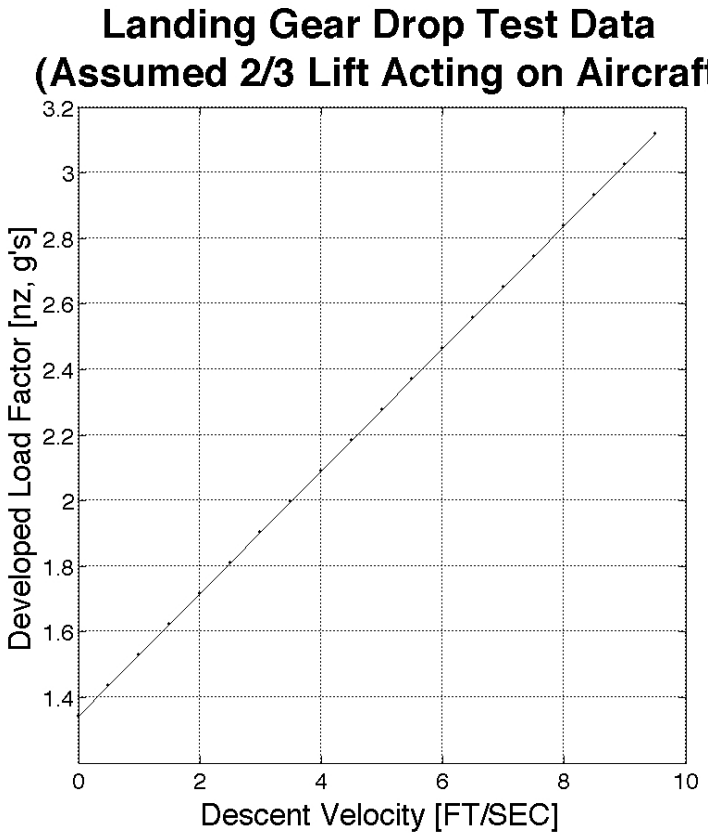

Figure 6 Landing Gear Drop Test Data [8]

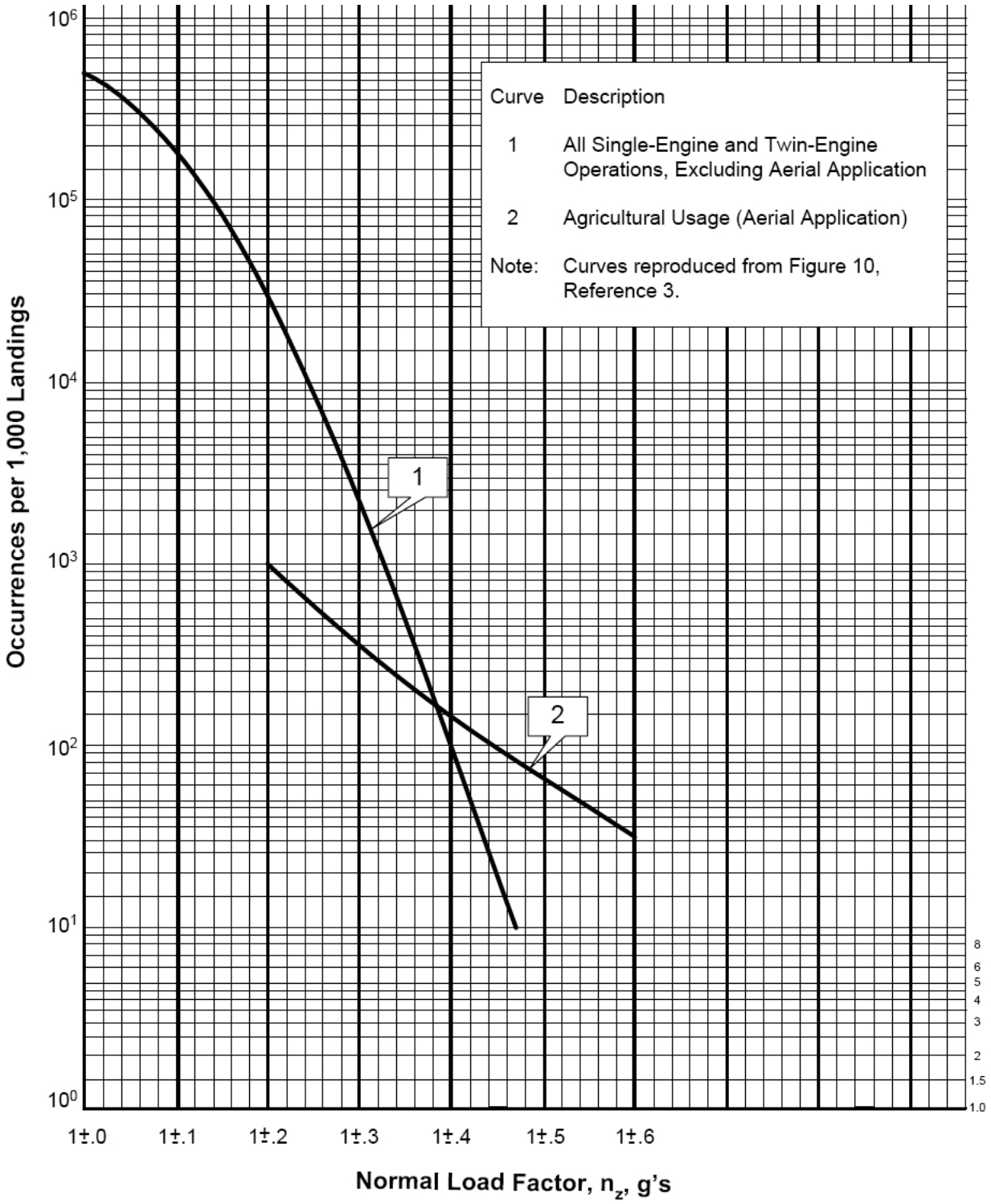

Figure 7 Exceedance Curve for Taxi

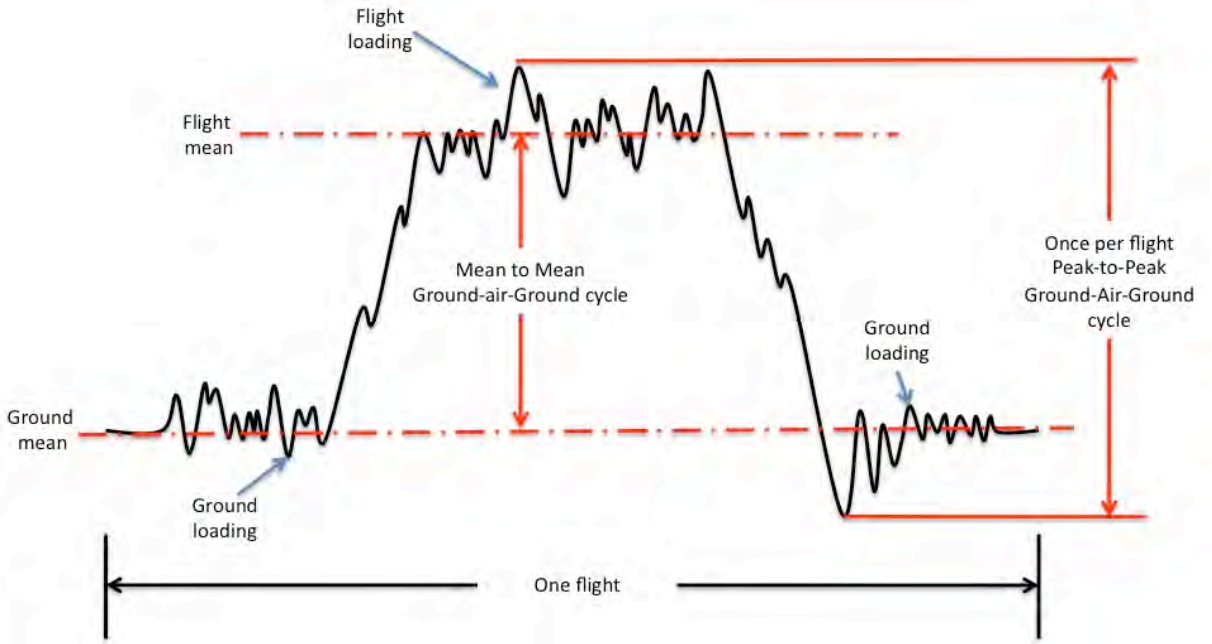

Figure 8 Ground-Air-Ground Cycle Schematic

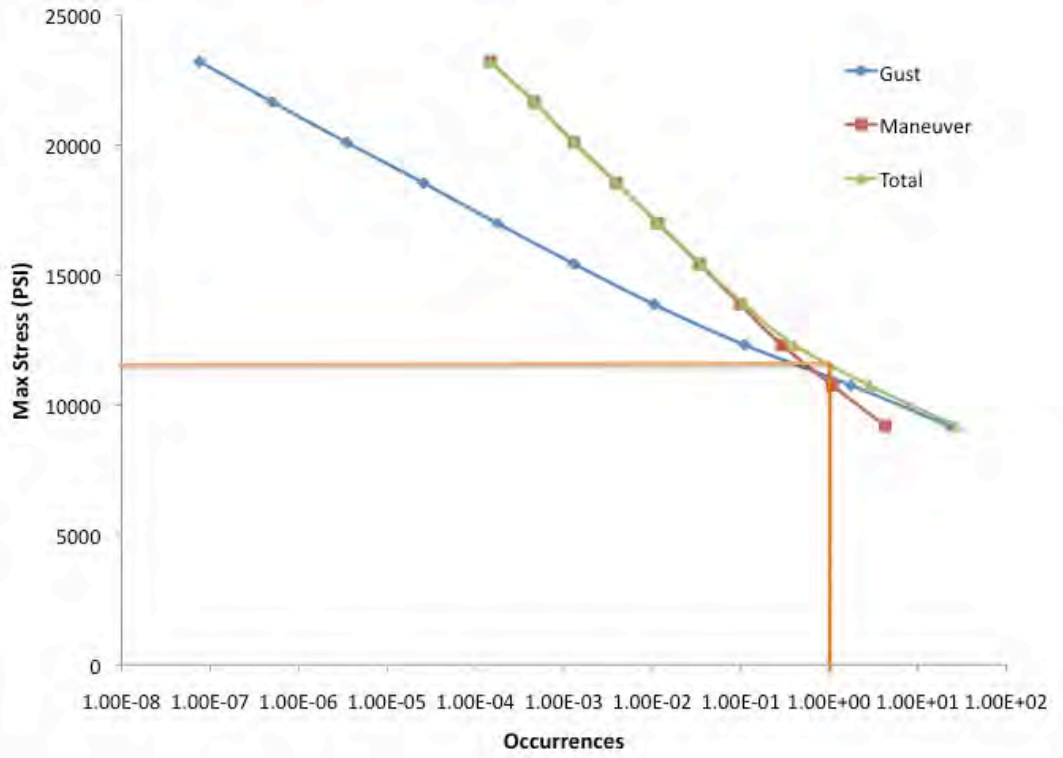

Figure 9 Ground-Air-Ground Example

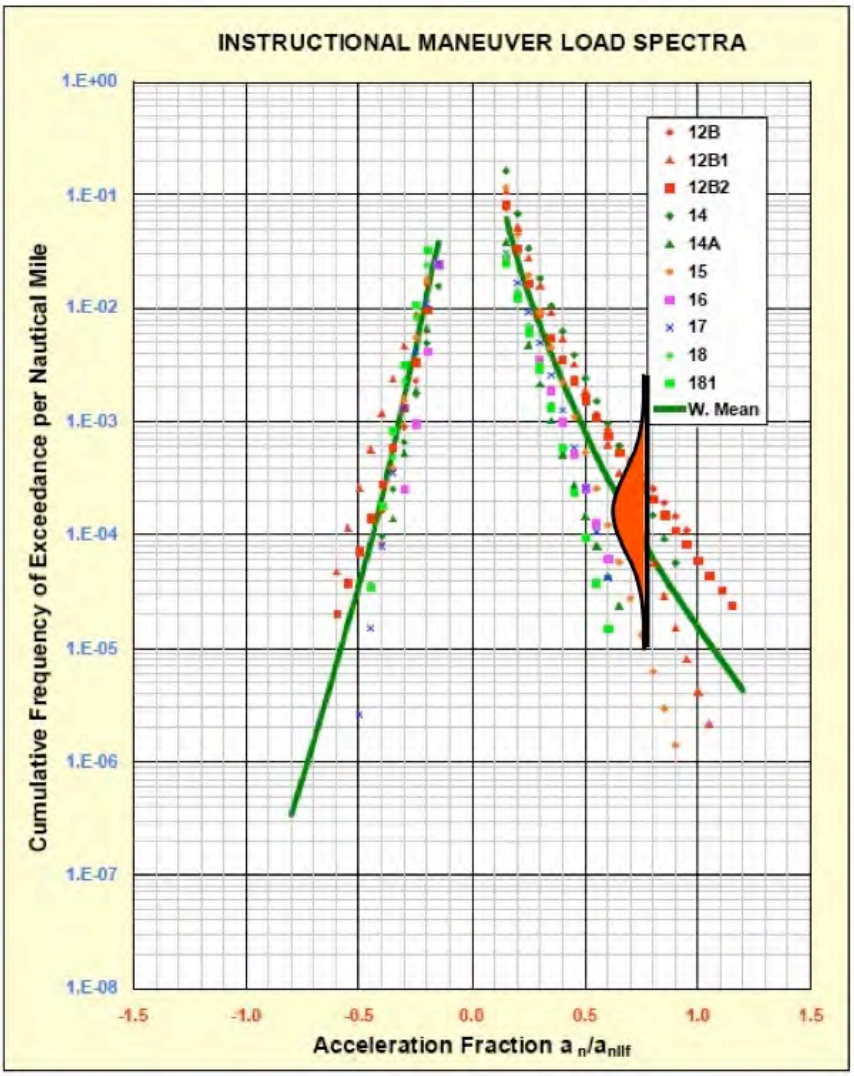

Figure 10. Random Maneuver Schematic Data

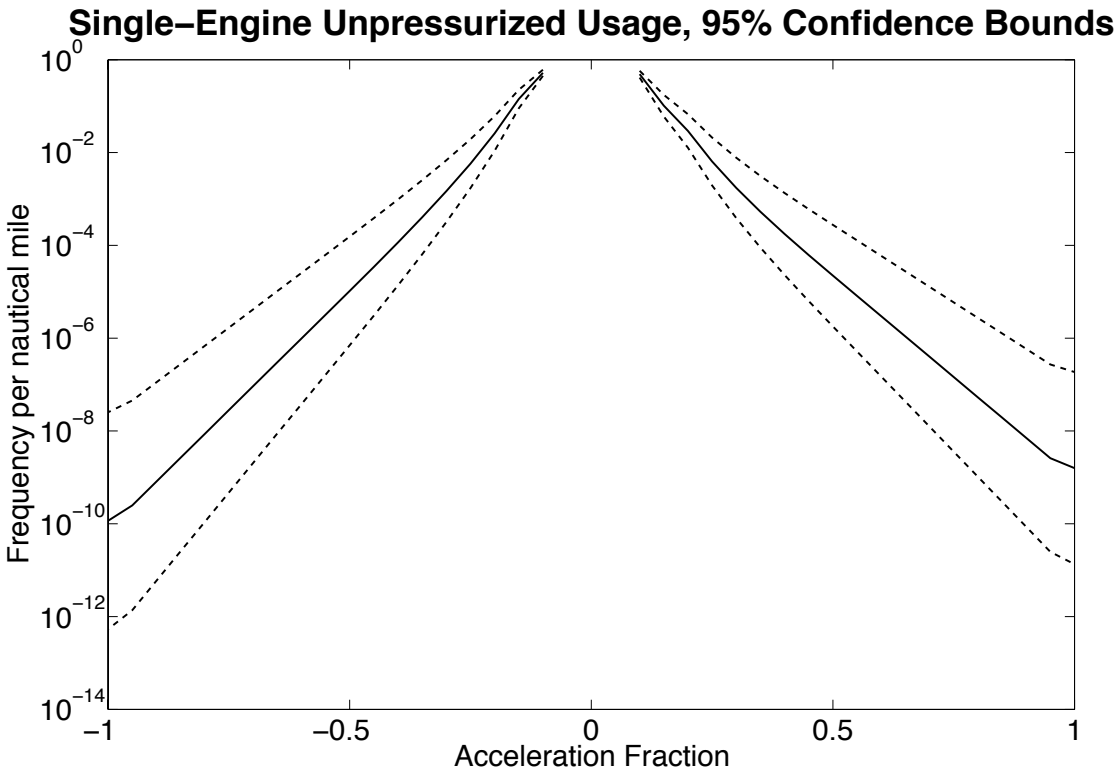

Figure 11. Random Gust Confidence Bounds Single-Engine Basic Instruction Usage

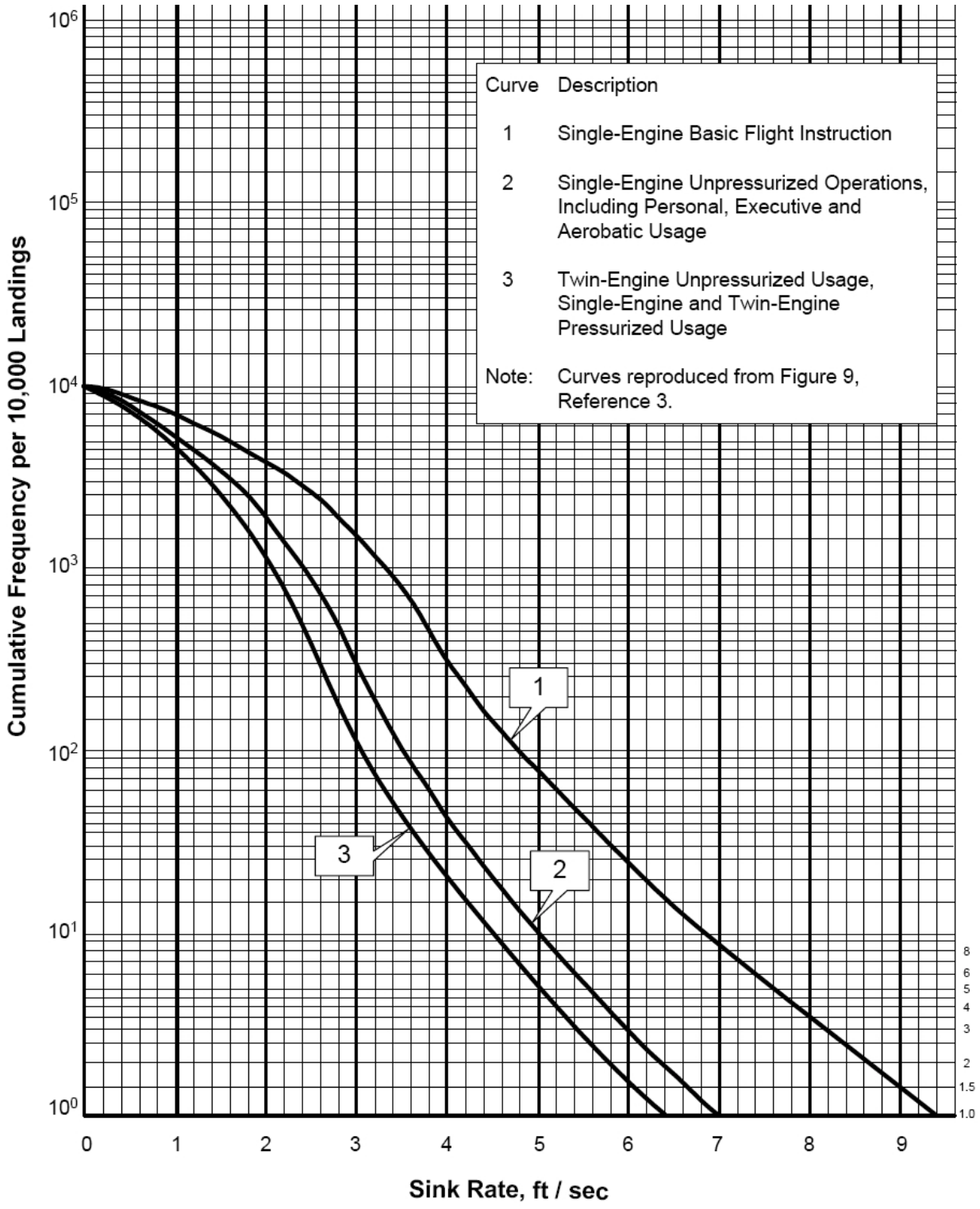

Figure 12. Landing Impact Spectra

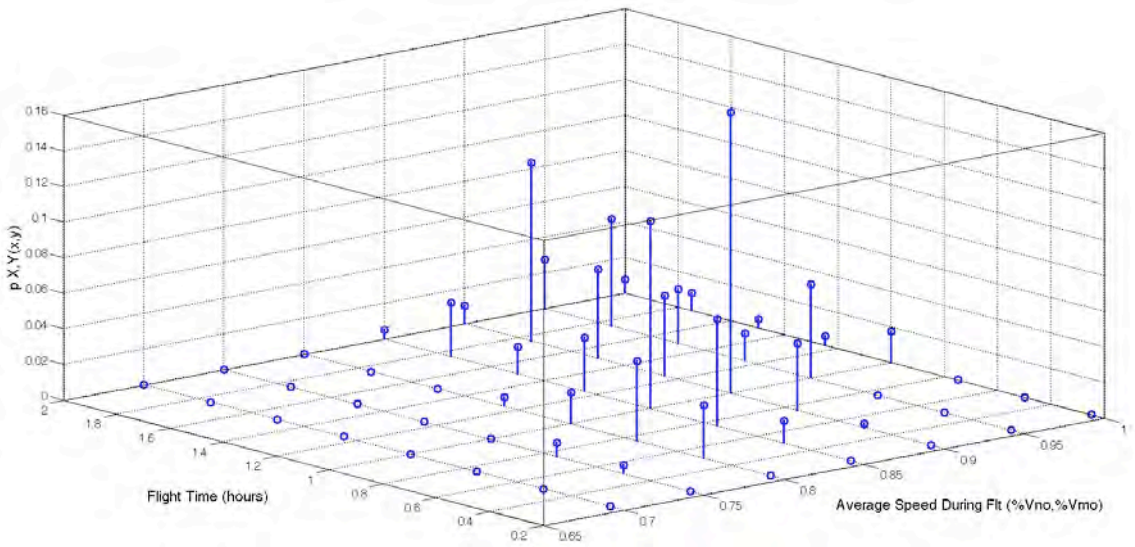

Figure 13. Flight Length and Airspeed Joint Probability Density Function

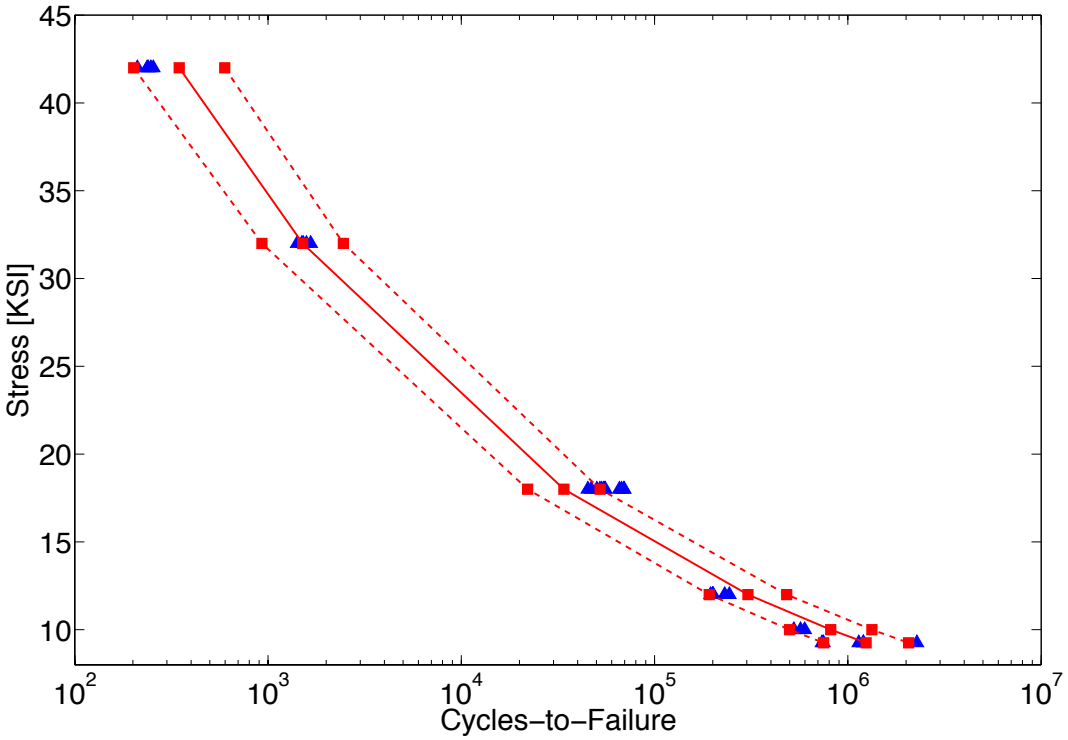

Figure 14. Open Hole 3 KSI Mean Stress Transfer (ASTM method)

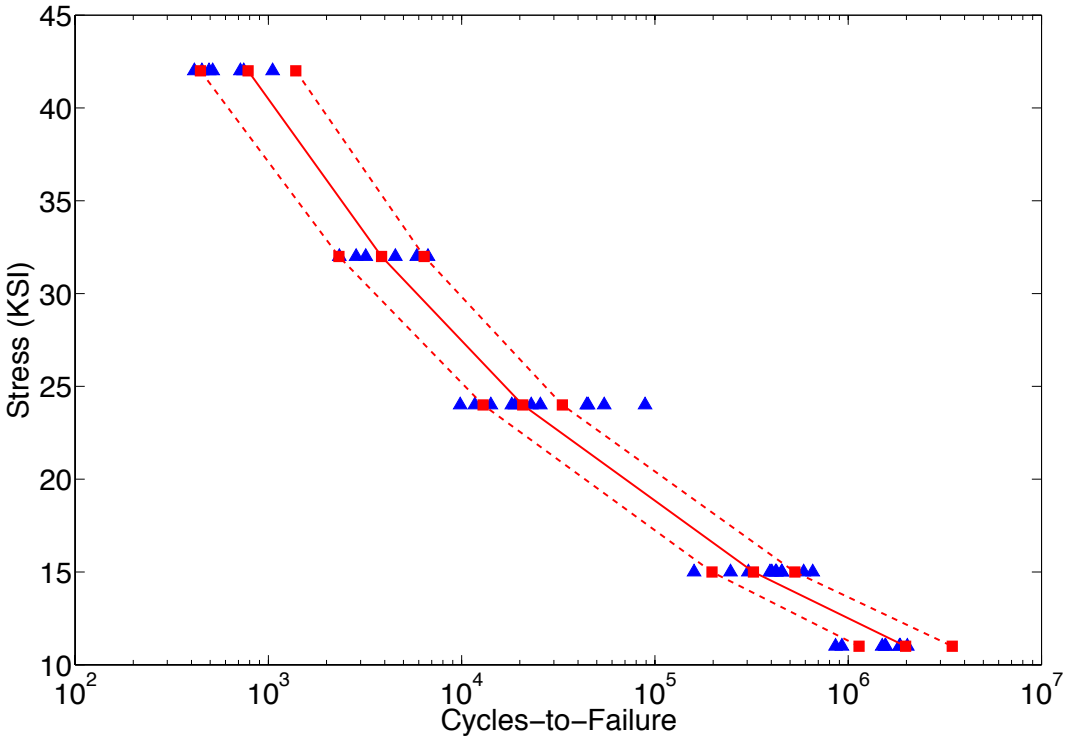

Figure 15. Hilok Fastener 6 KSI Mean Stress 50% Load (ASTM method)

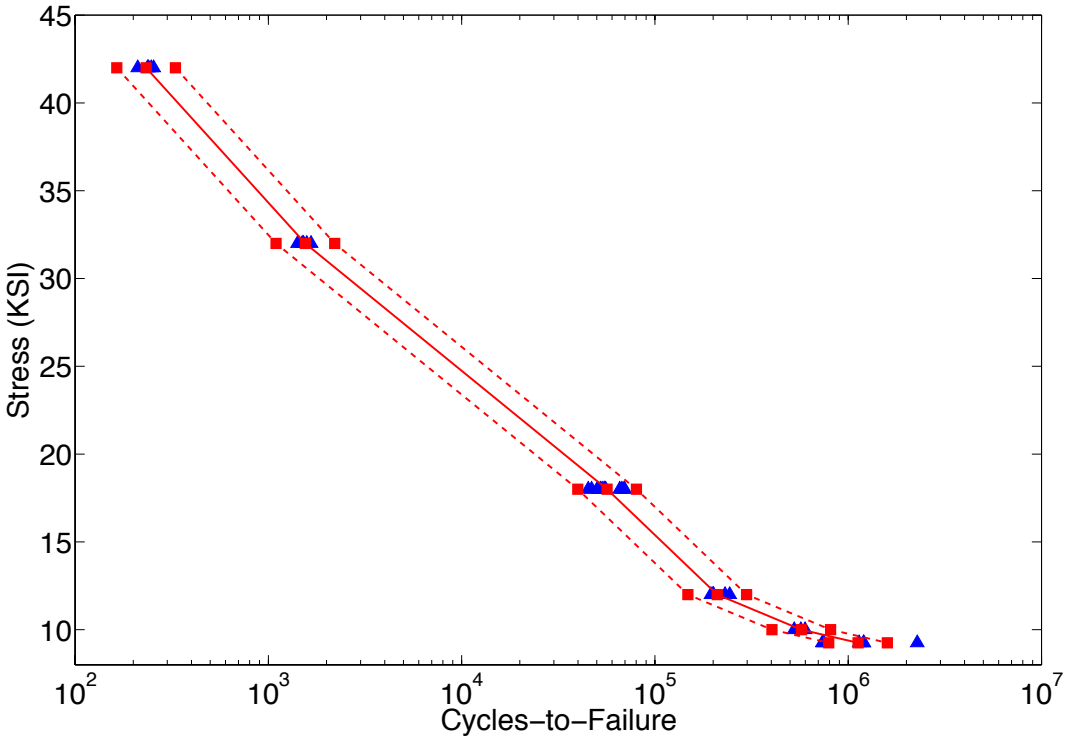

Figure 16. Open Hole 3 KSI Mean Stress Transfer (Polynomial method)

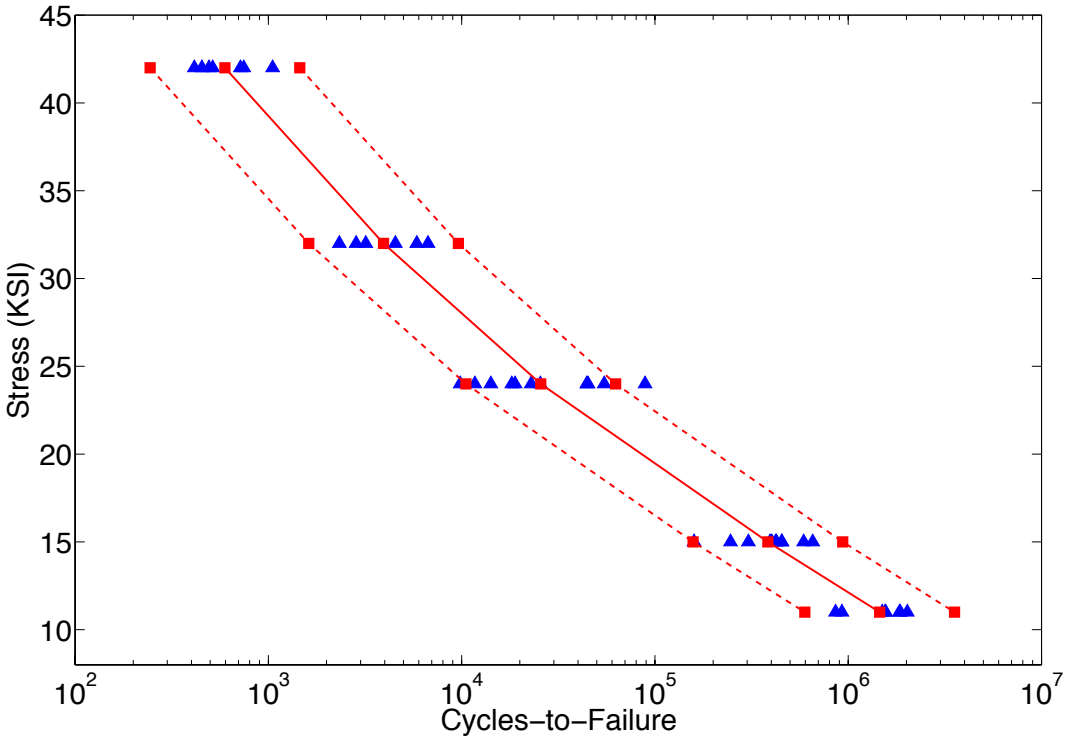

Figure 17. Hilok Fastener 6 KSI Mean Stress 50% Load (Polynomial method)

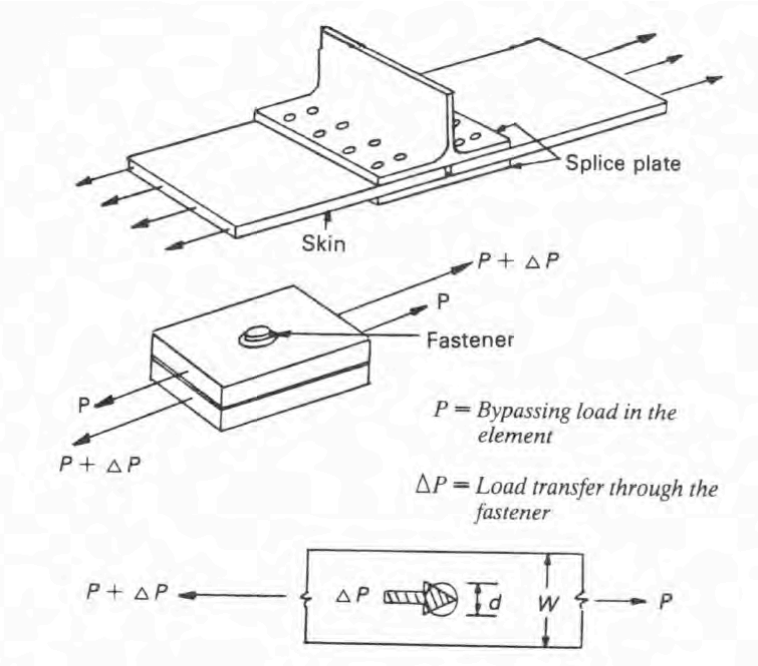

Figure 18. Load Fastener, Load Transfer, and Bypass Load [13]

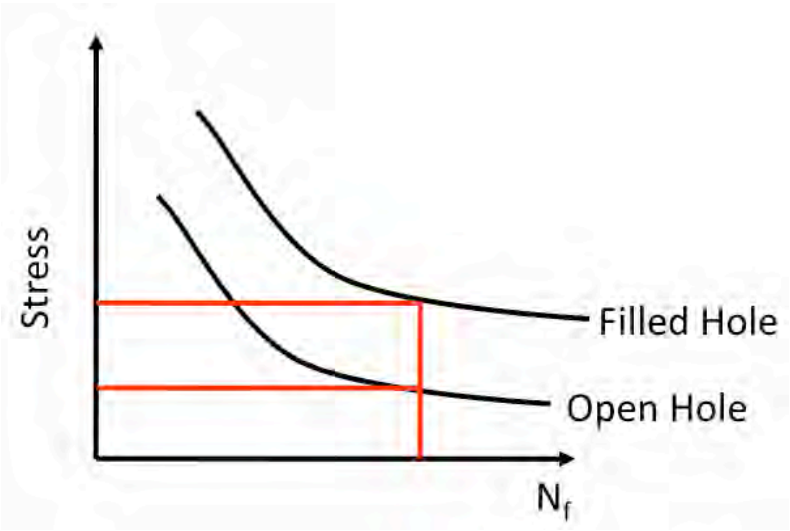

Figure 19. Beta and Theta Graphical Calculation

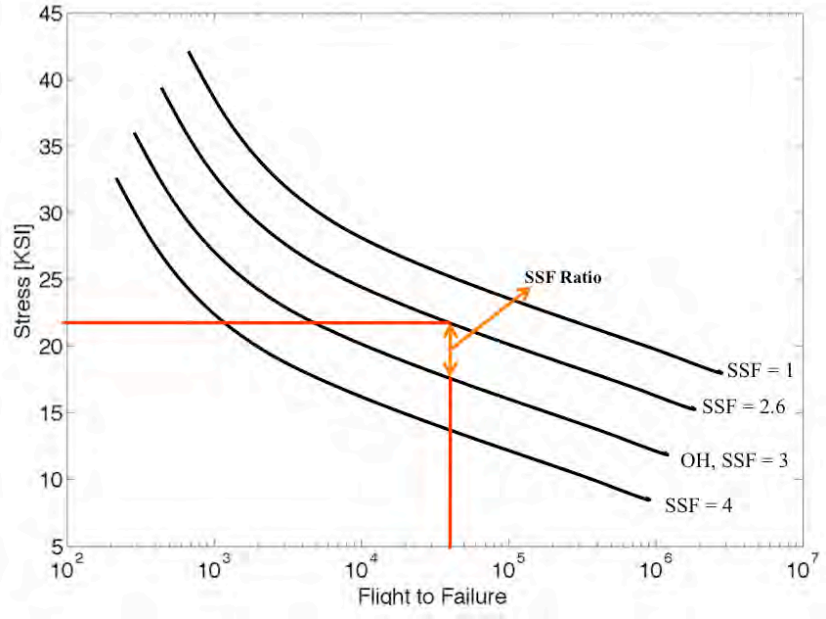

Figure 20. SN Prediction Using Open Hole Data and SSF

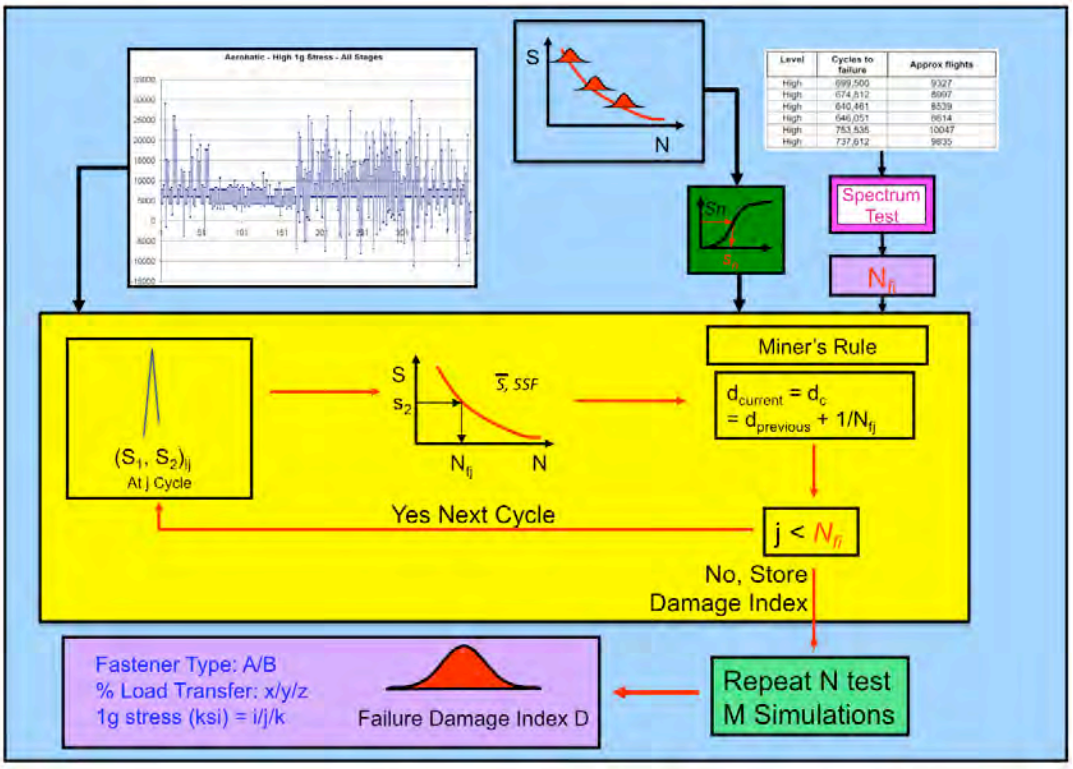

Figure 21. Random Miner's Damage Index Accumulation Flowchart

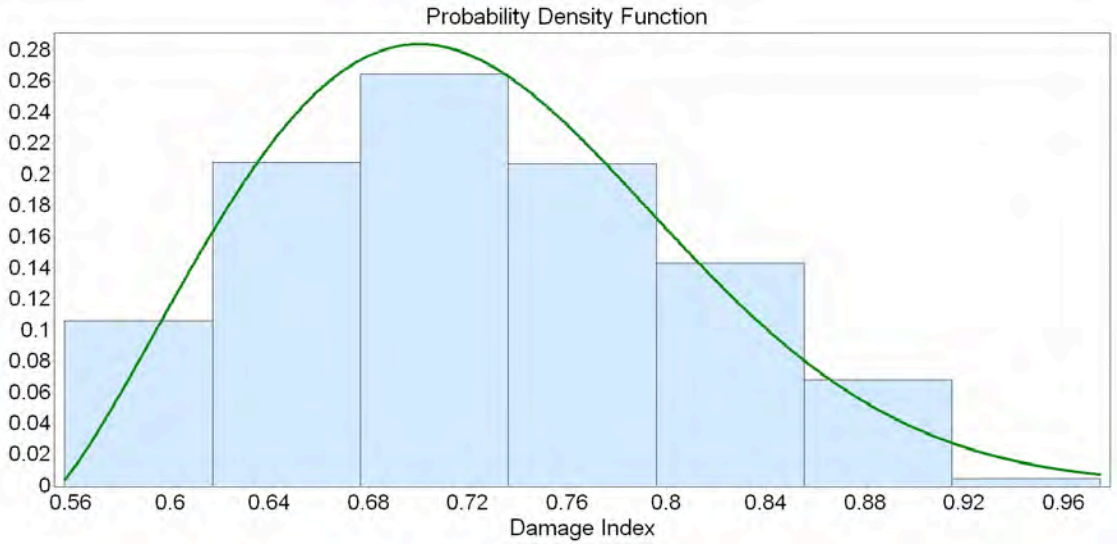

Figure 22. Probability Density Function Normal Usage, High Severity, and Open Hole

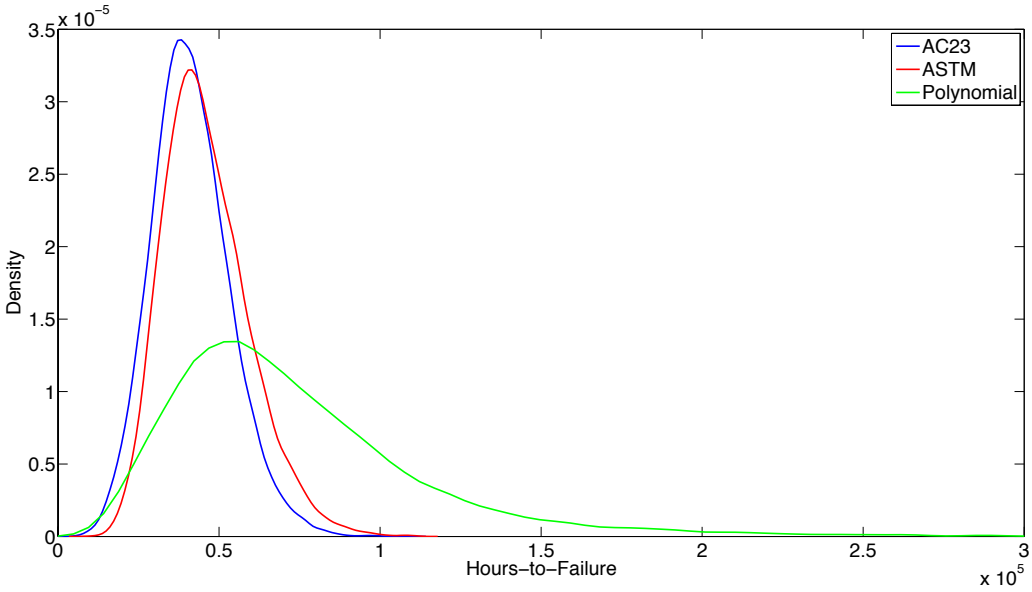

Figure 23. Flights-to-Failure Probability Density Function

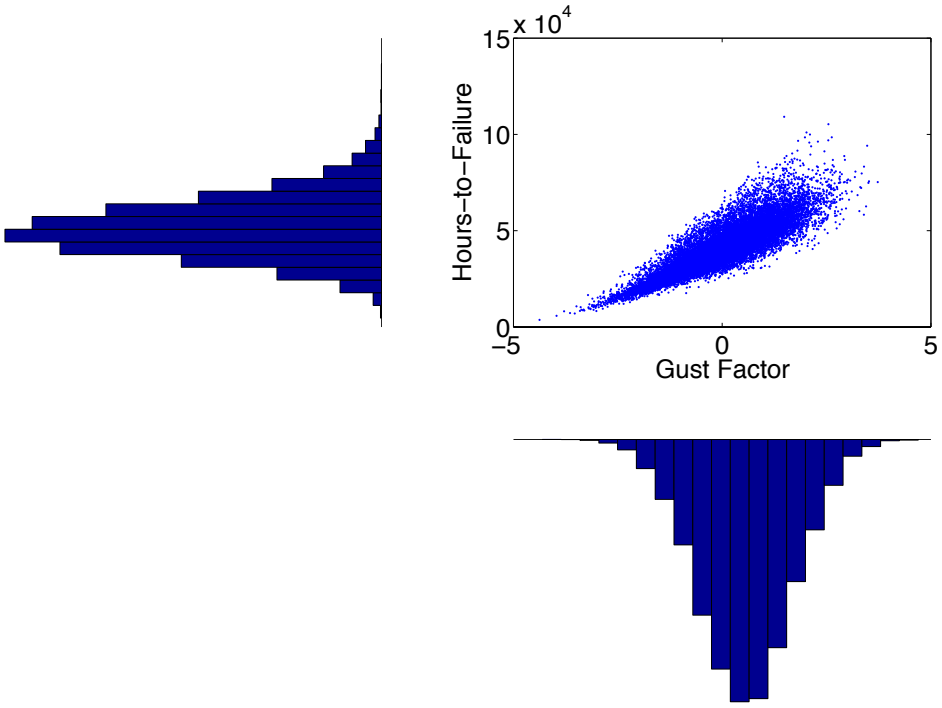

Figure 24. Scatter Plot Hours-to-Failure Versus Gust Factor (AC23 SN Curve)

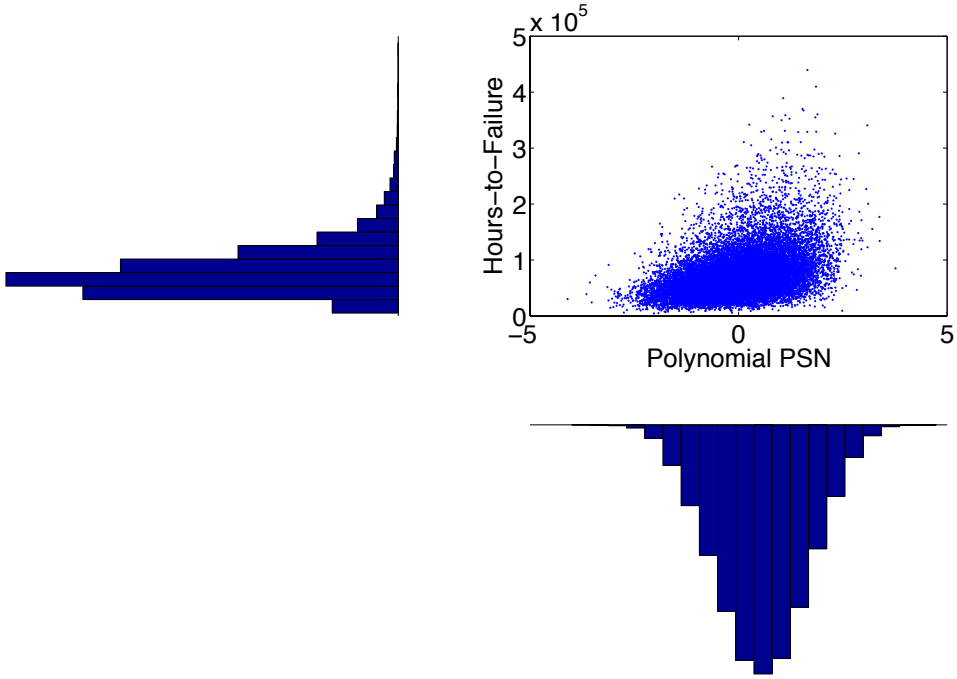

Figure 25. Scatter Plot Hours-to-Failure Versus PSN Curve (Polynomial SN Curve)

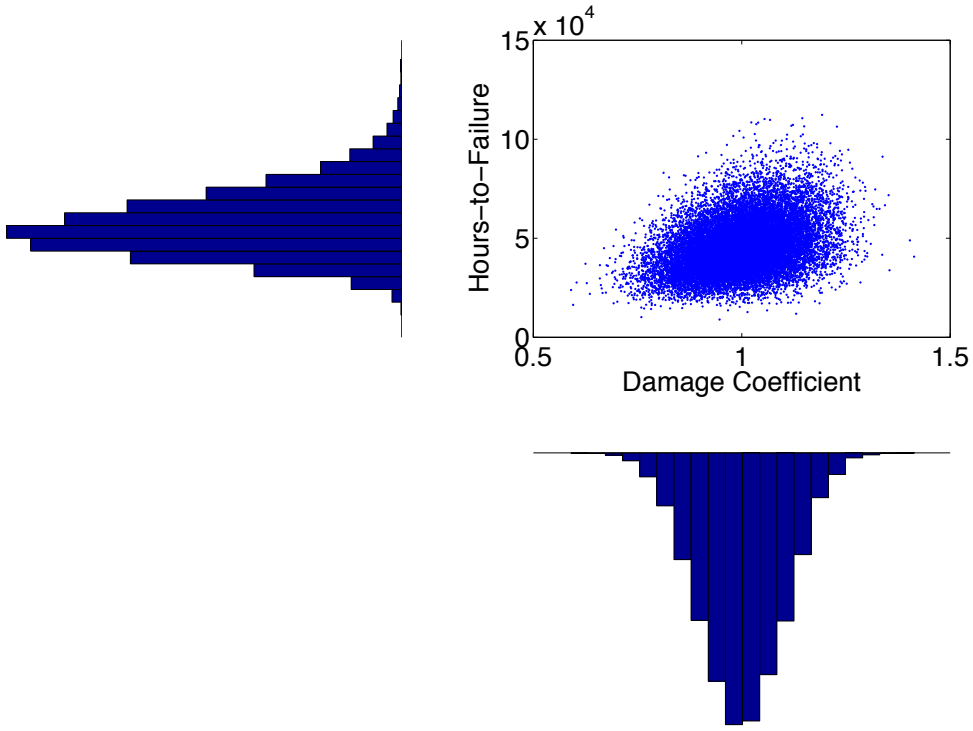

Figure 26. Scatter Plot Hours-to-Failure Versus Miners Damage Coefficient (ASTM SN Curve)

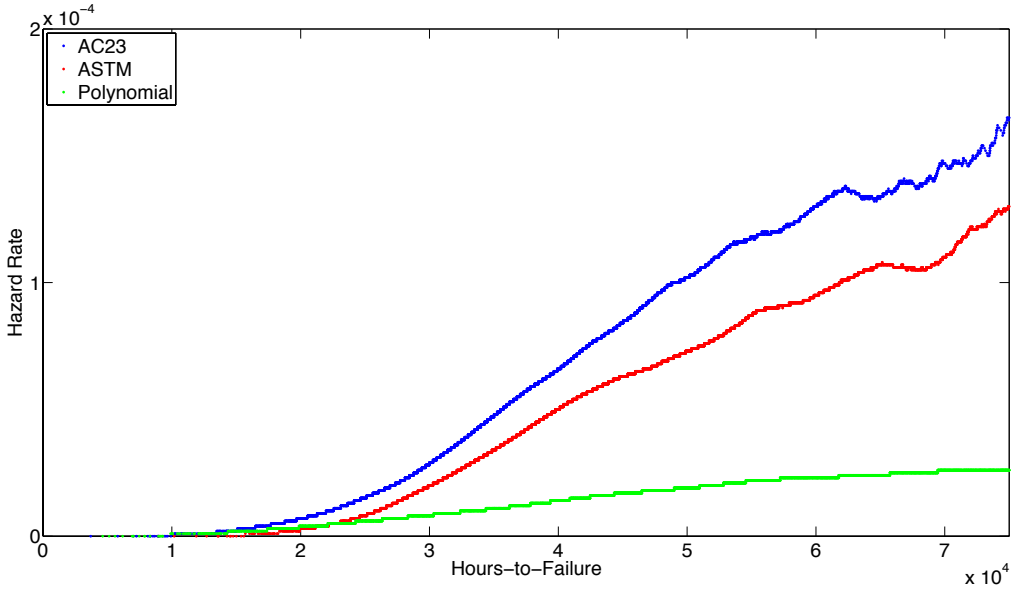

Figure 27. Hazard function ASTM Curve

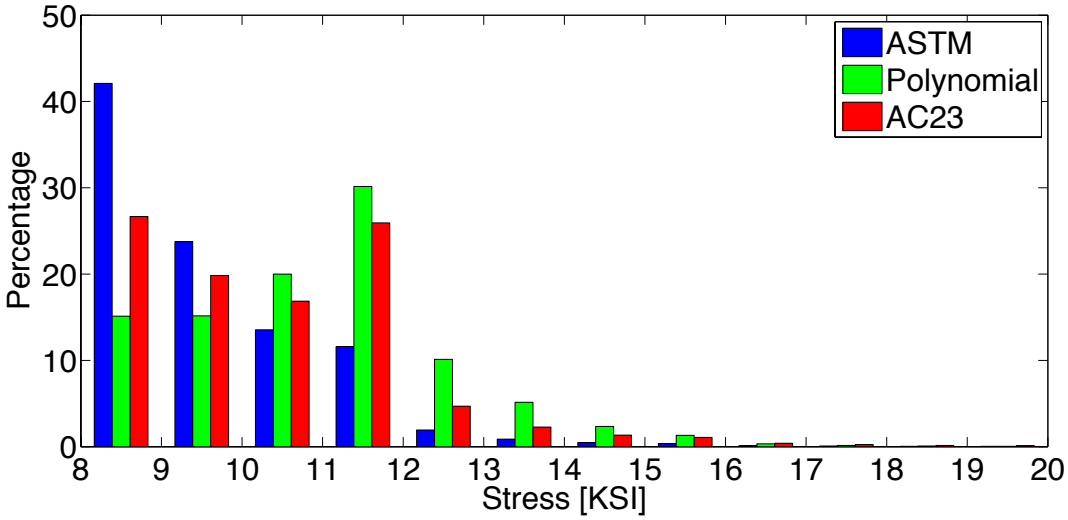

Figure 28. PSN Region Cumulated Damage

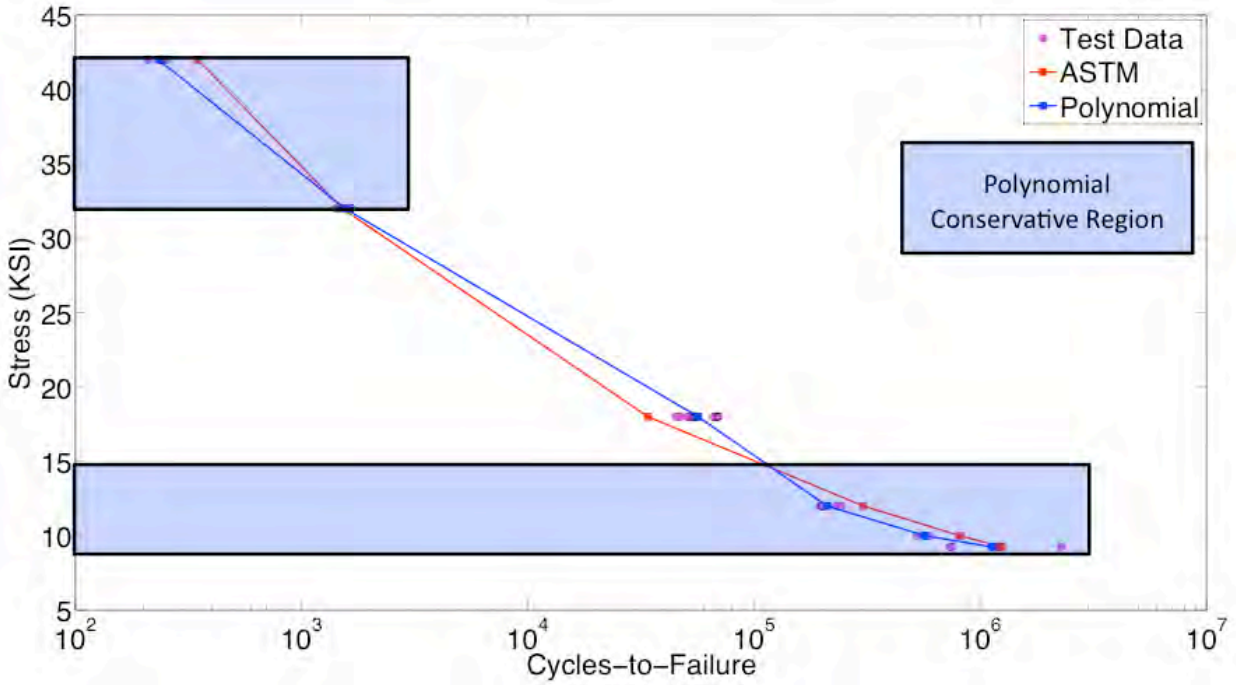

Figure 29. PSN Comparison

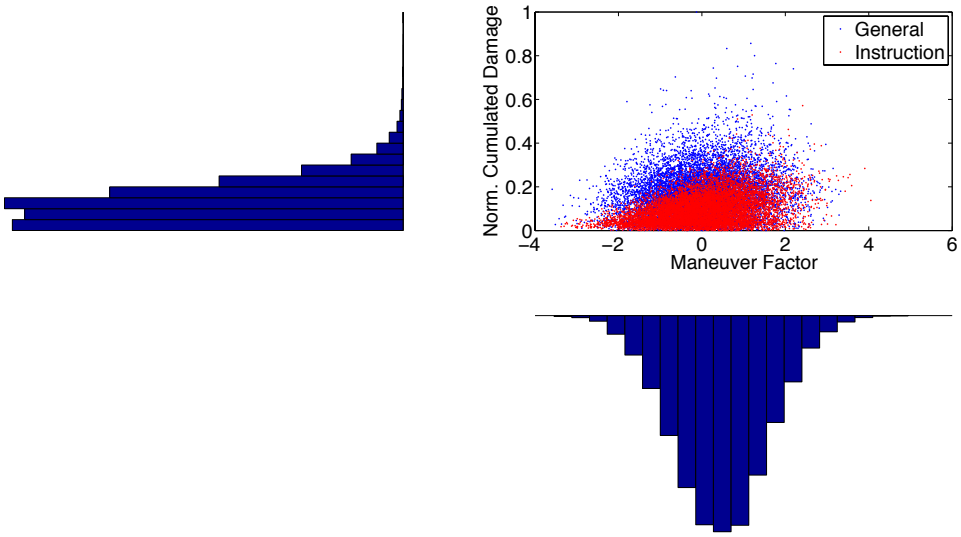

Figure 30. Scatter Plot Normalized Cumulated Damage Versus Maneuver Factor

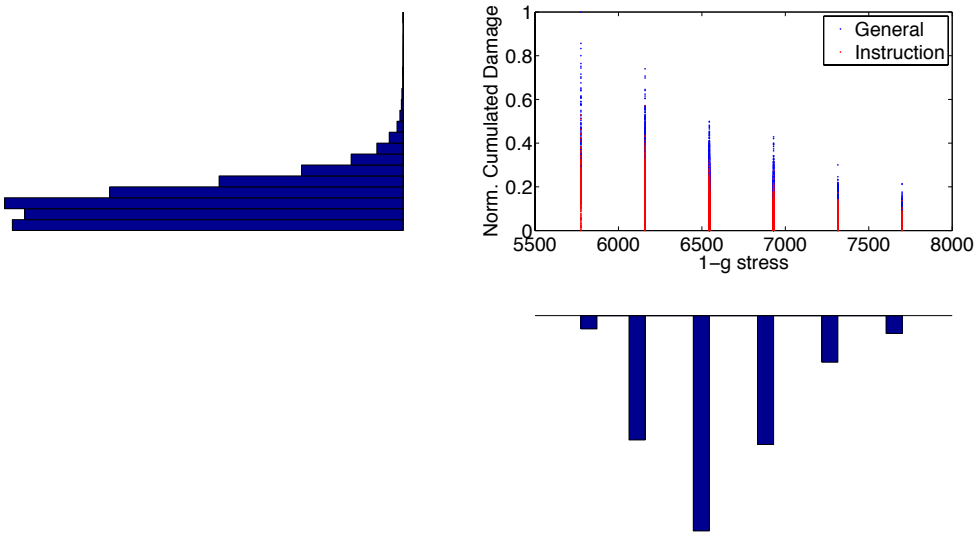

Figure 31. Scatter Plot Normalized Cumulated Damage Versus 1g Stress

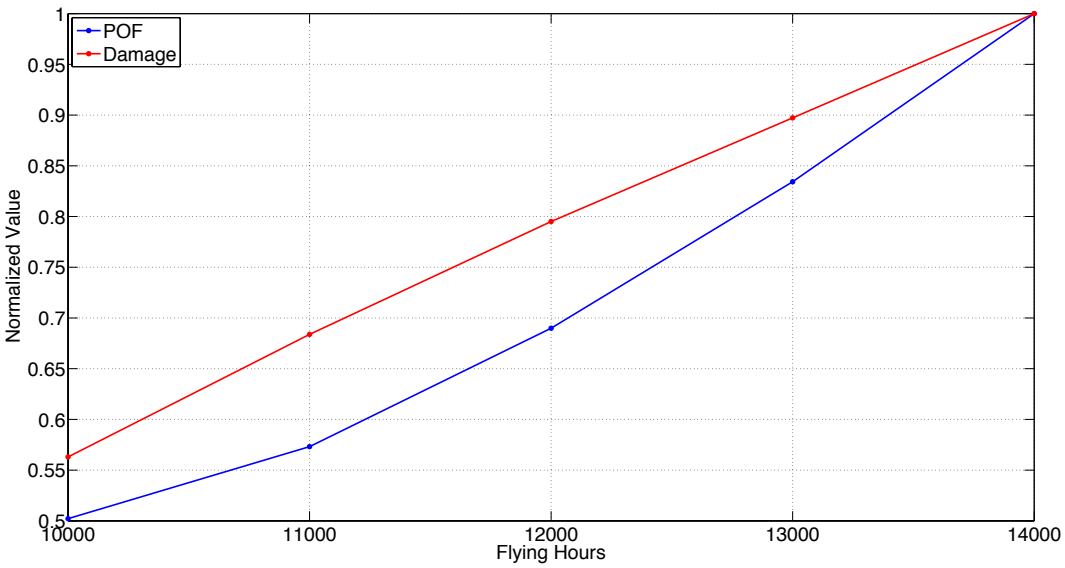

Figure 32. Normalized cumulative Damage and Probability of Failure

LIST OF FIGURES

Figure Page

LIST OF TABLES